

Development of novel salicylic acid derivatives with dual anti-inflammatory and anti-arthritic potentials: Synthesis, *in vitro* bio-evaluation, and *in-silico* toxicity prediction with molecular modeling simulations

Kholoud Hesham ¹, Wael M. Aboulthanab ², Ahmed Ragab ^{3,4,*}

¹ Nanoscience & Technology Program, Faculty of Science, Galala University, Galala City, 43511, Suez, Egypt

² Biochemistry Department, Biotechnology Research Institute, National Research Centre, Dokki 12622, Cairo, Egypt

³ Chemistry Department, Faculty of Science, Galala University, Galala City, 43511, Suez, Egypt

⁴ Chemistry Department, Faculty of Science (boys), Al-Azhar University, 11884 Nasr City, Cairo-Egypt

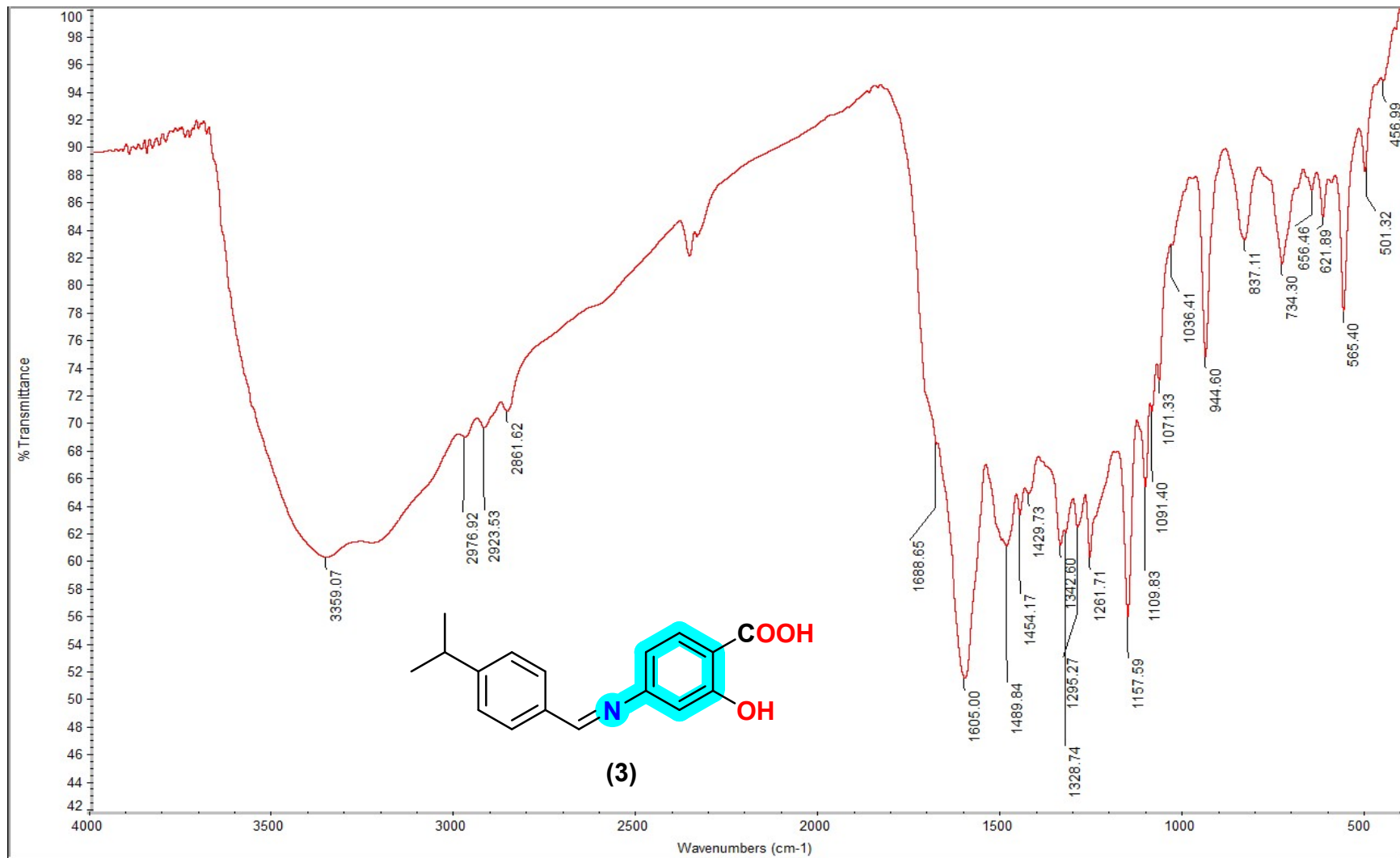


Figure (1): IR spectrum of compound 3

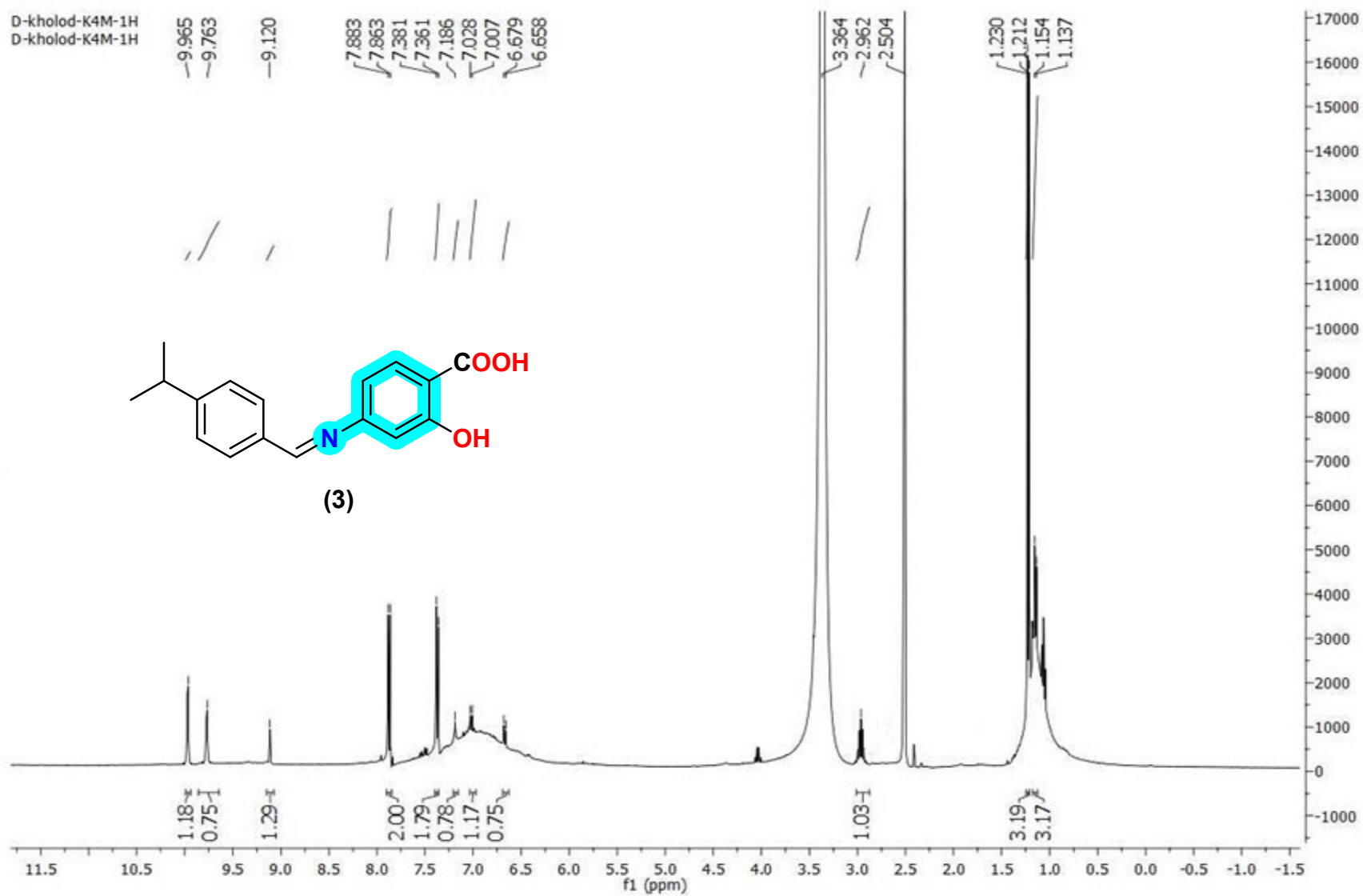


Figure (2): H NMR spectrum of compound 3

D-kholod-K4-c13
D-kholod-K4-c13

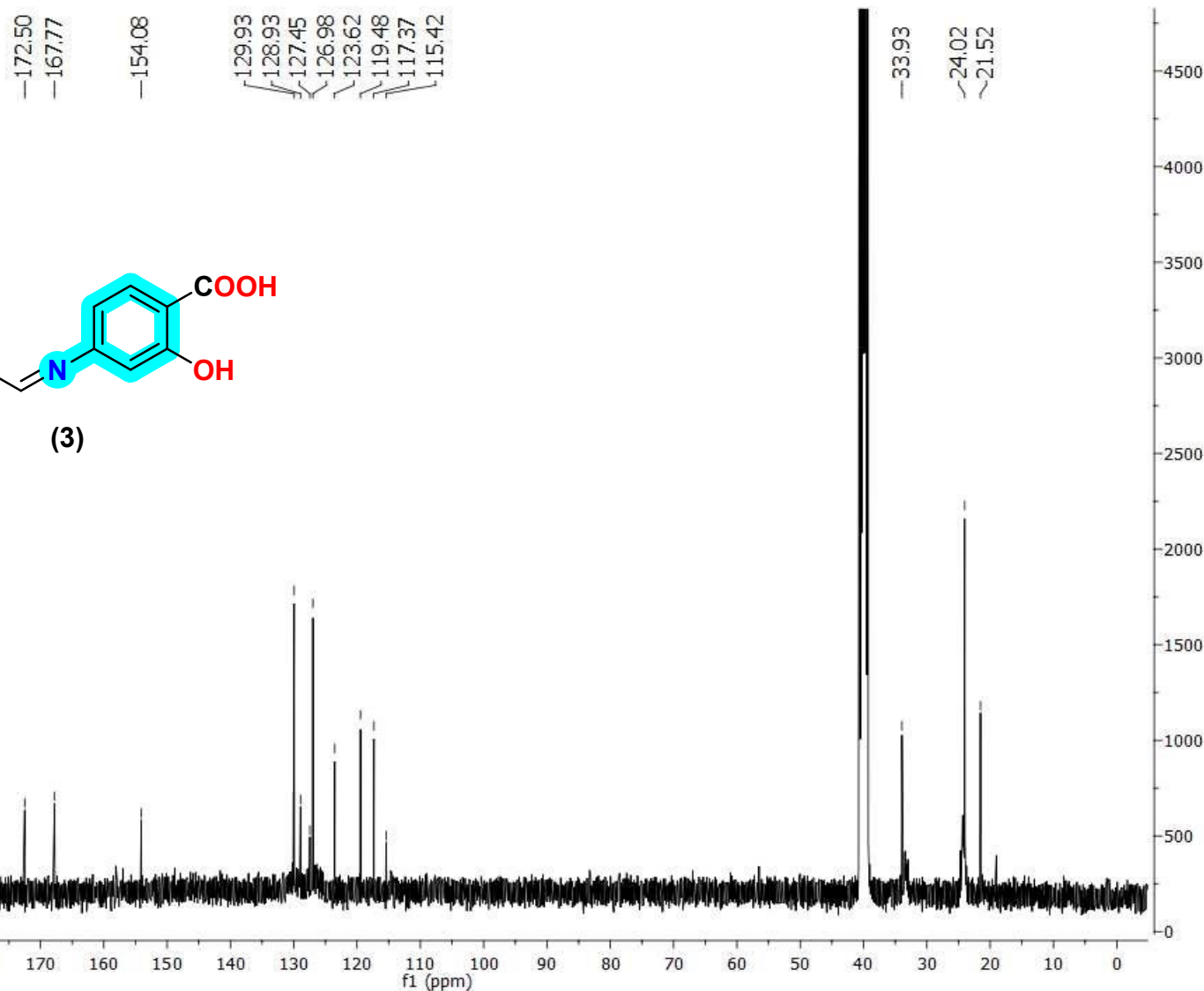


Figure (3): ¹³C NMR spectrum of compound 3

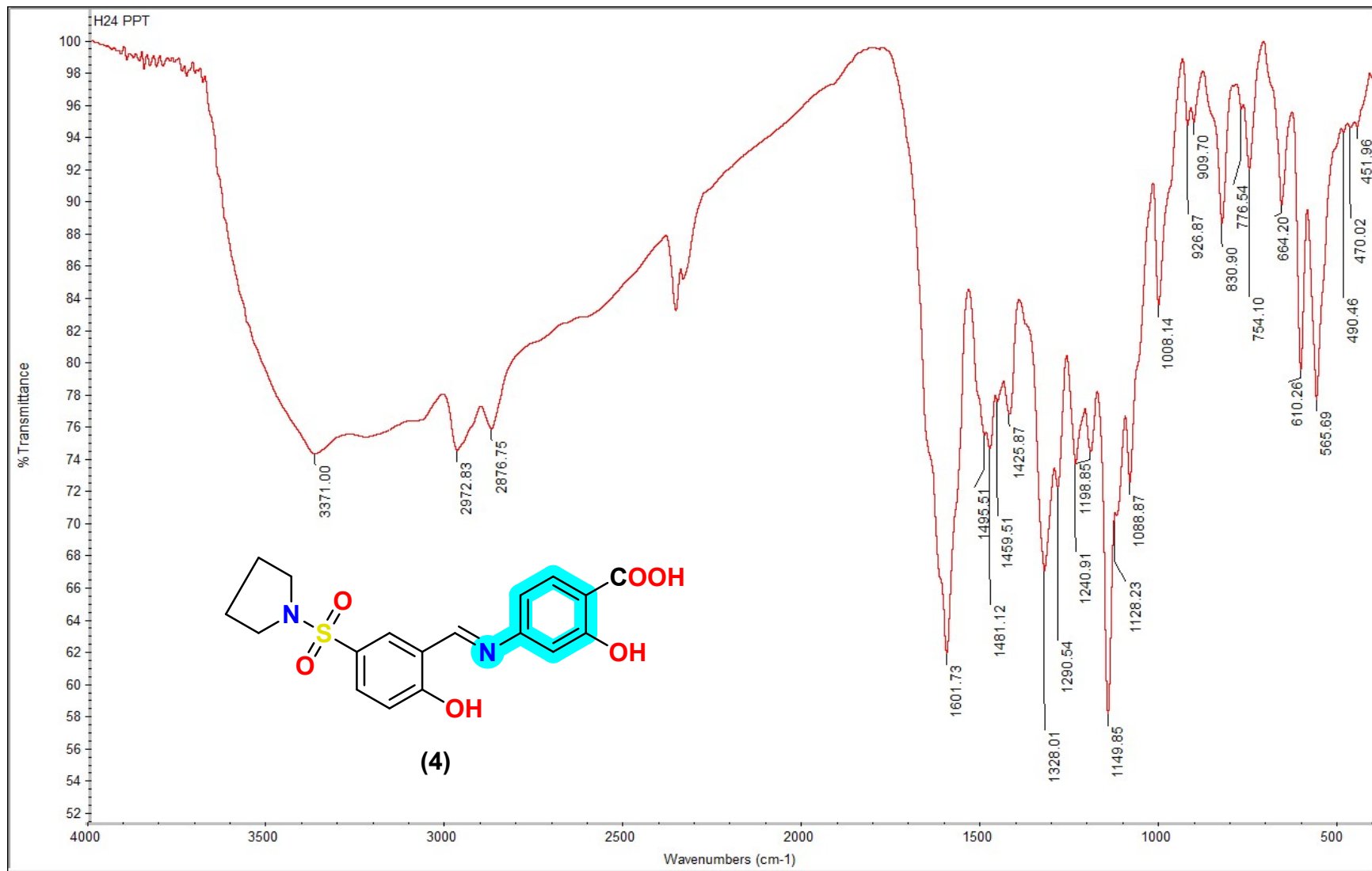


Figure (4): IR spectrum of compound 4

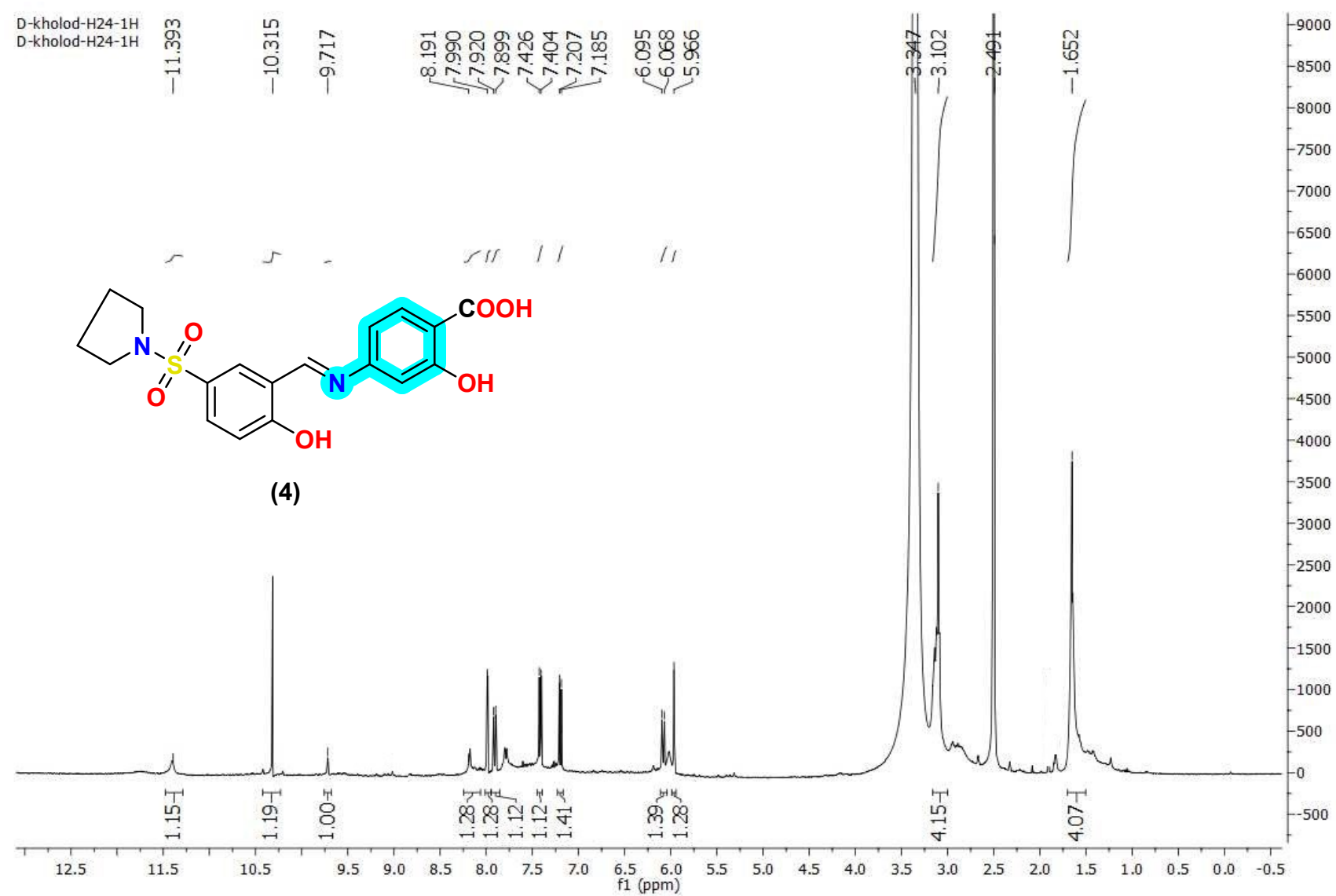


Figure (5): ^1H NMR spectrum of compound 4

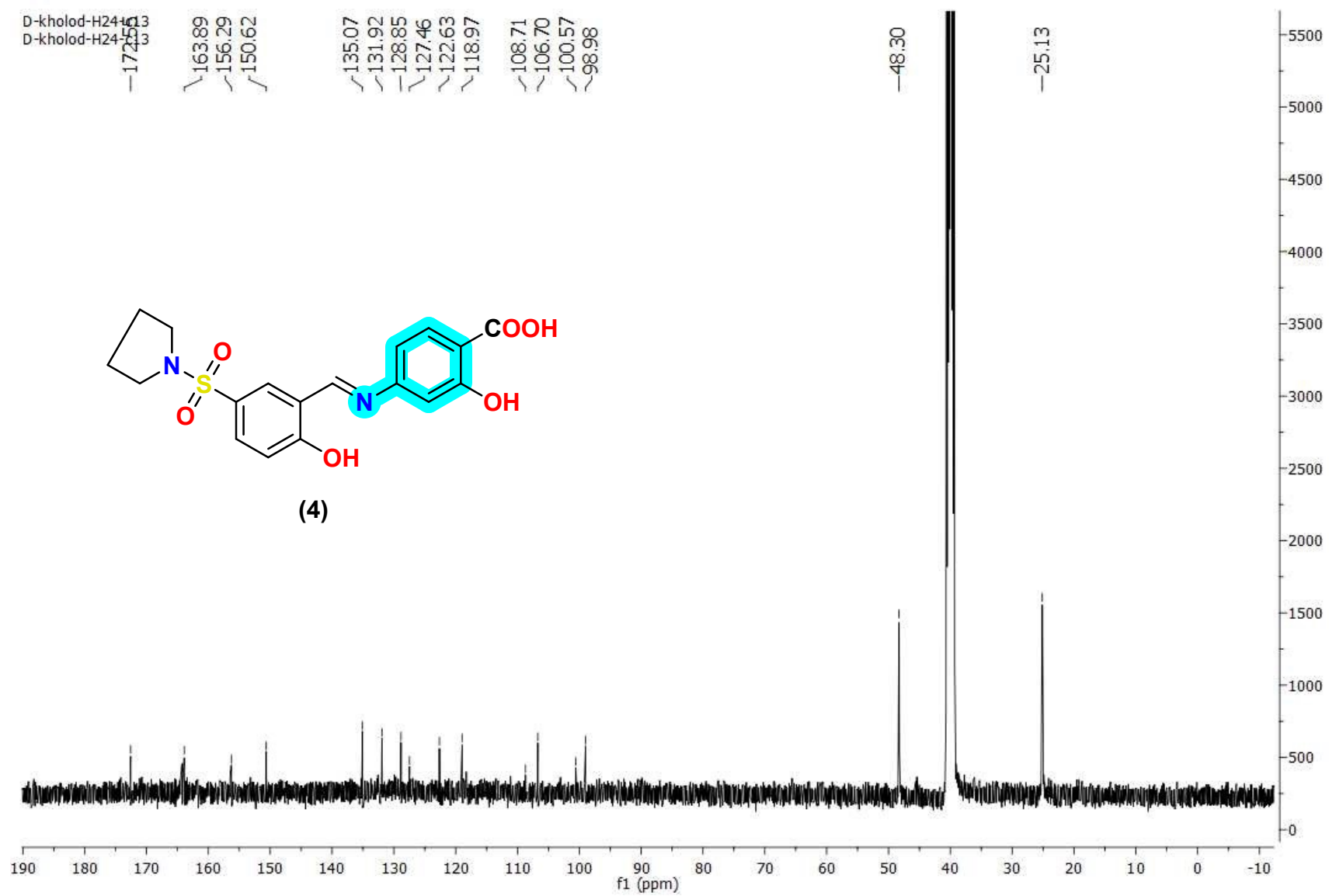


Figure (6): ^{13}C NMR spectrum of compound 4

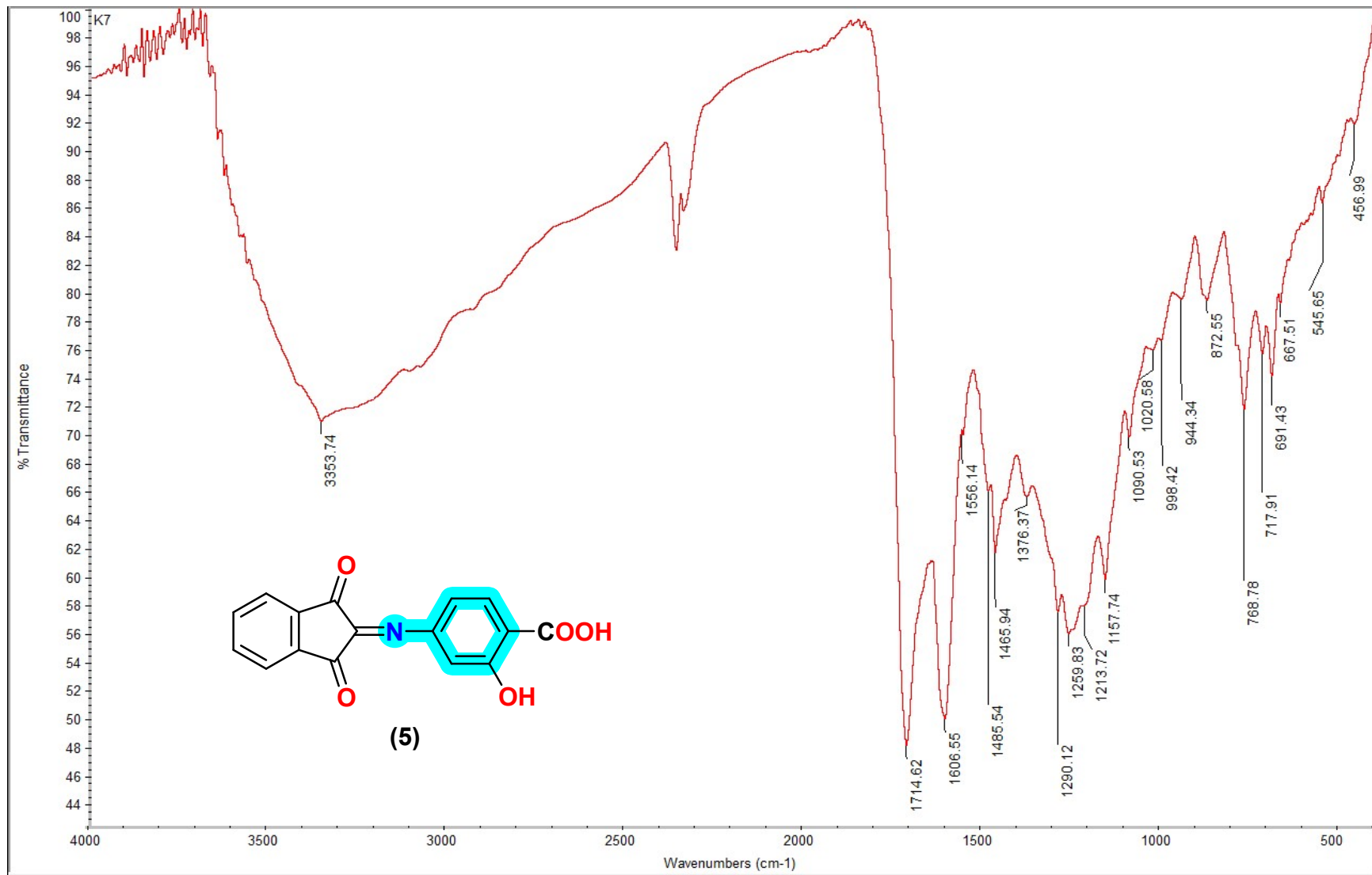


Figure (7): IR spectrum of compound 5

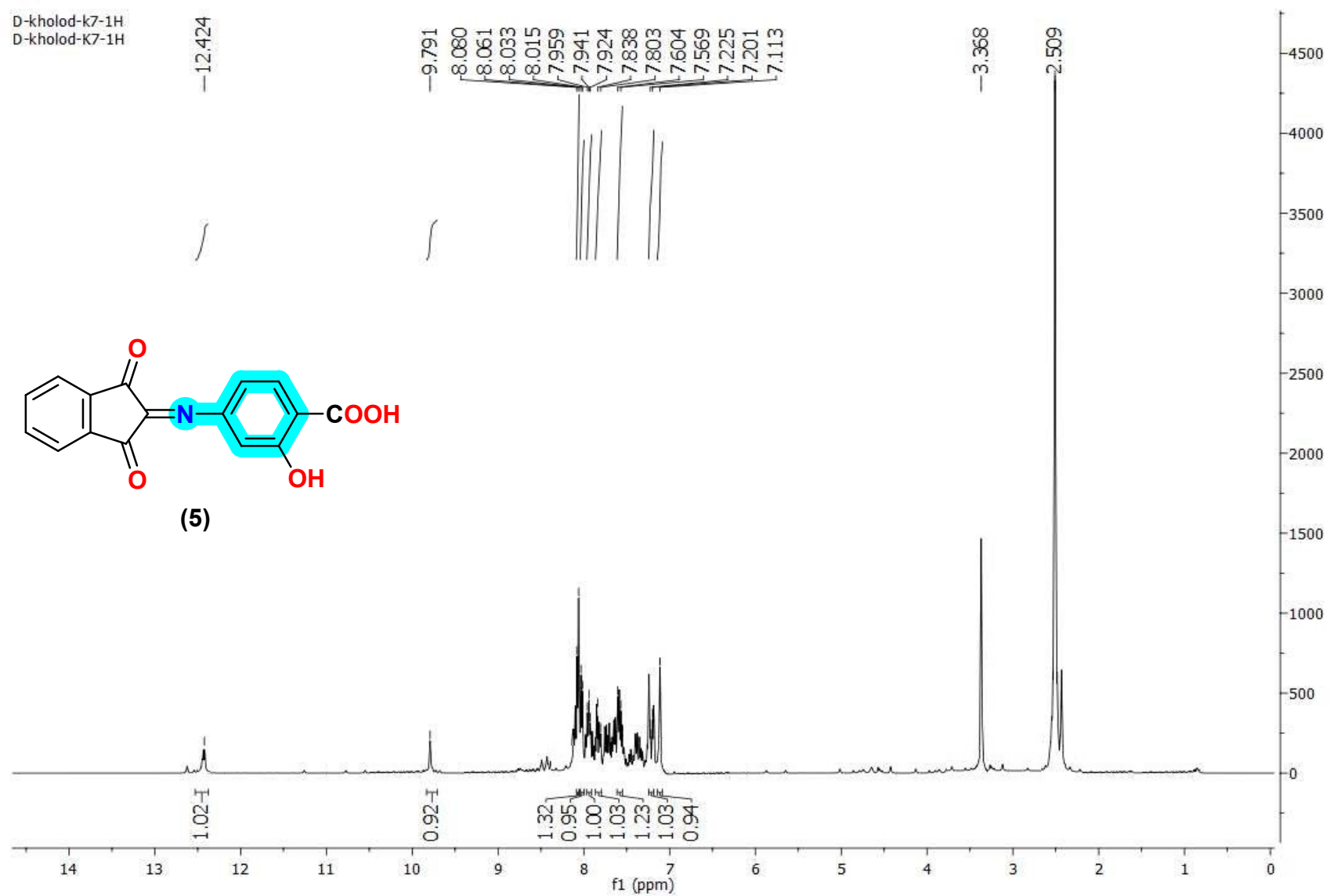


Figure (8): ^1H NMR spectrum of compound 5

D-kholod-k7-c13
D-kholod-K7-c13

~174.06
~172.50

-158.00

140.80
137.08
135.29
131.45
129.73
124.75
123.83
110.57
110.21
106.62

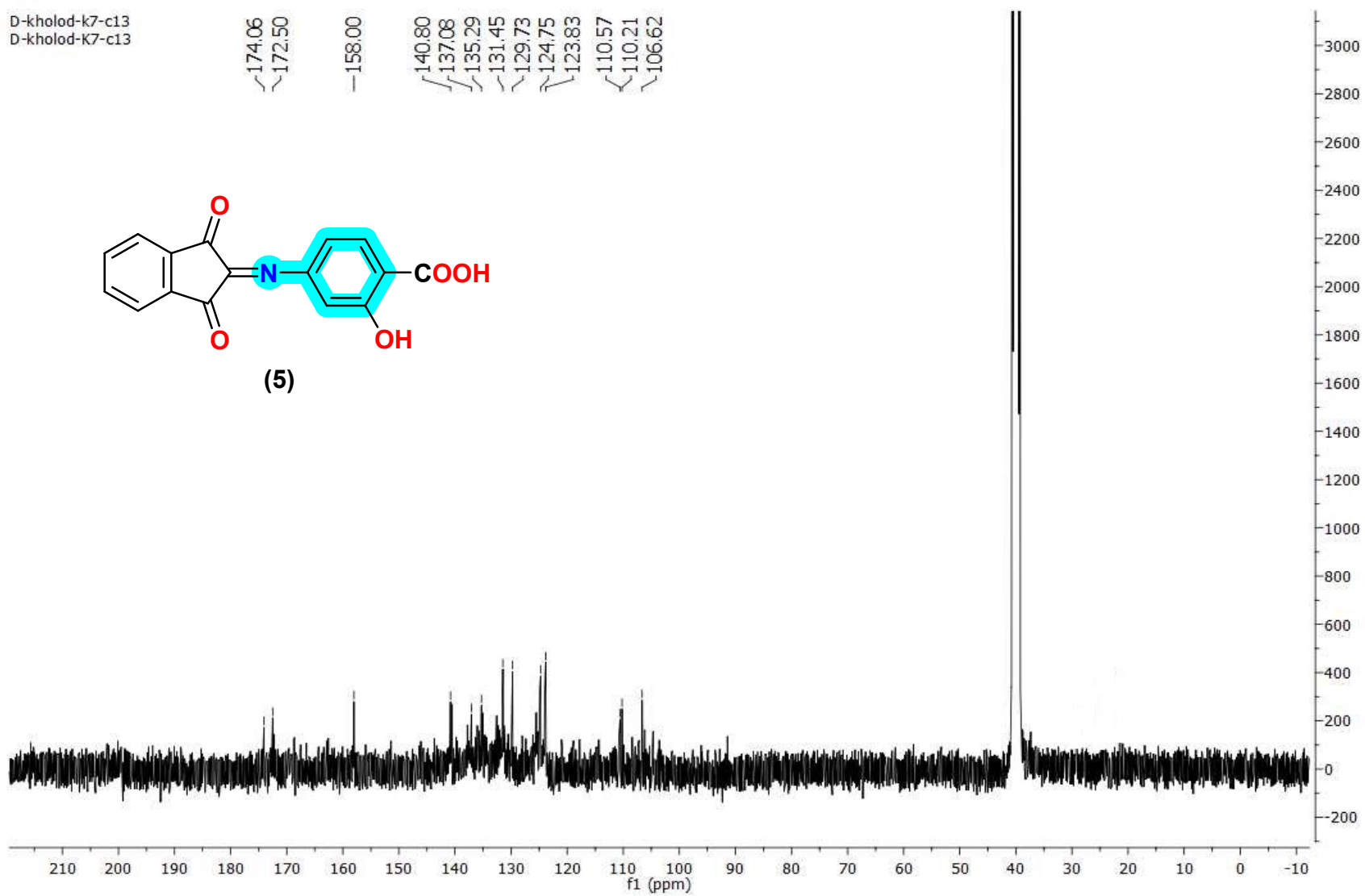
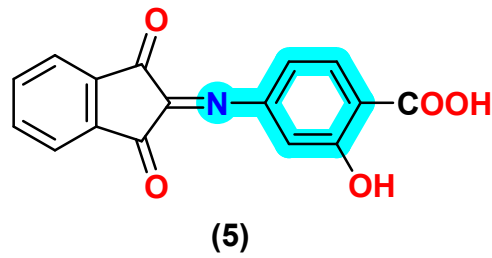


Figure (9): ^{13}C NMR spectrum of compound 5

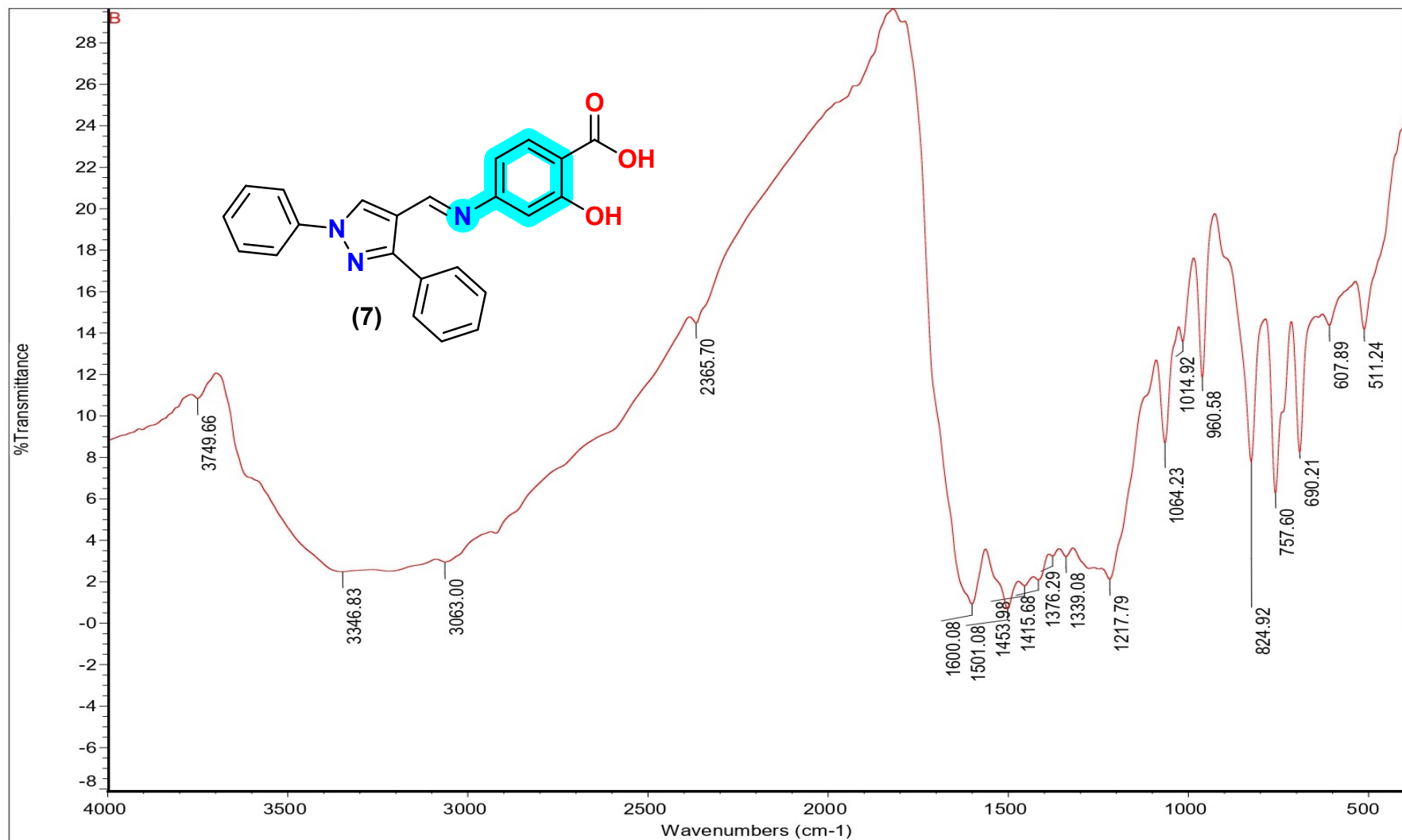
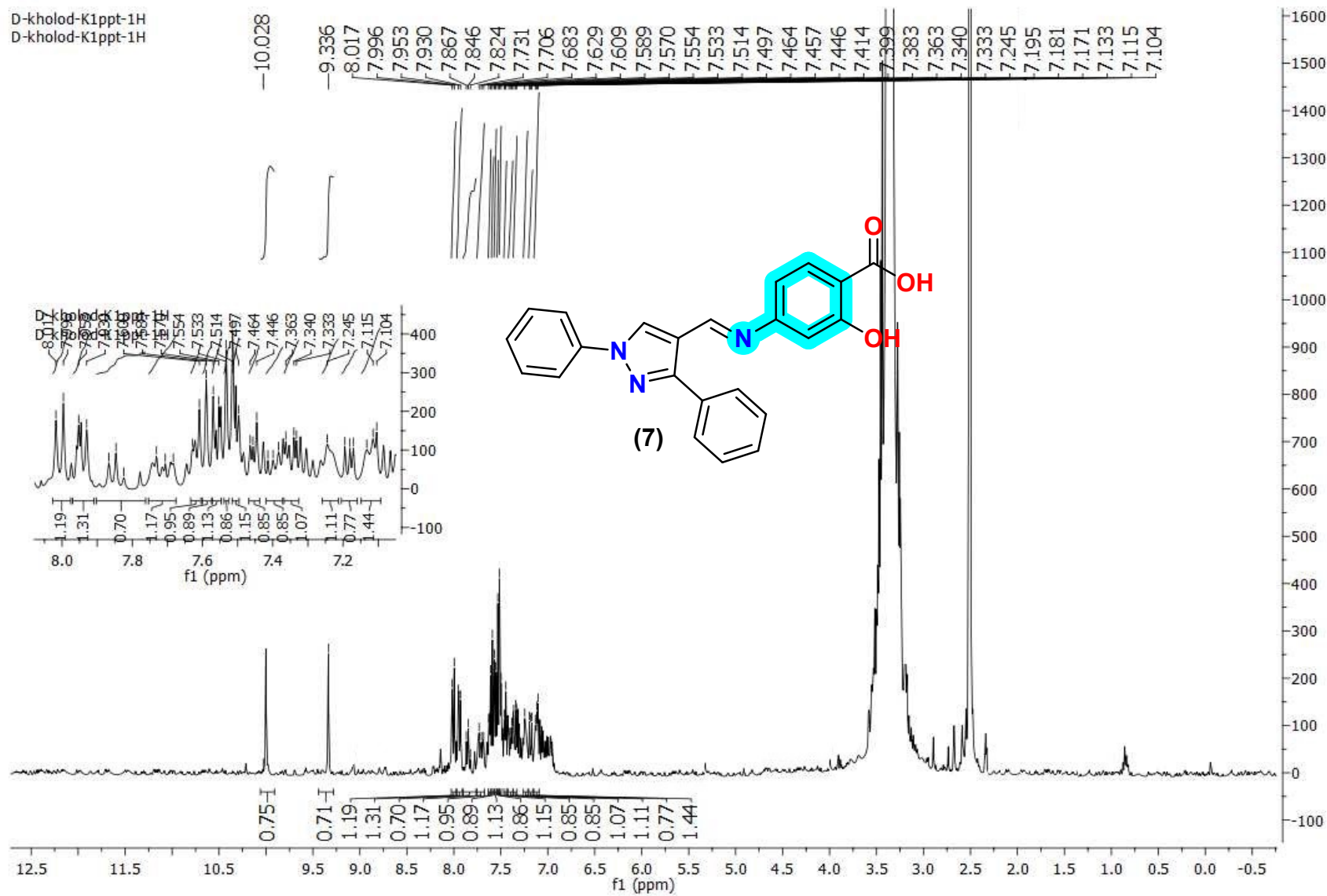


Figure (10): IR spectrum of compound 7



D-kholod-K1-c13
D-kholod-K1-c13

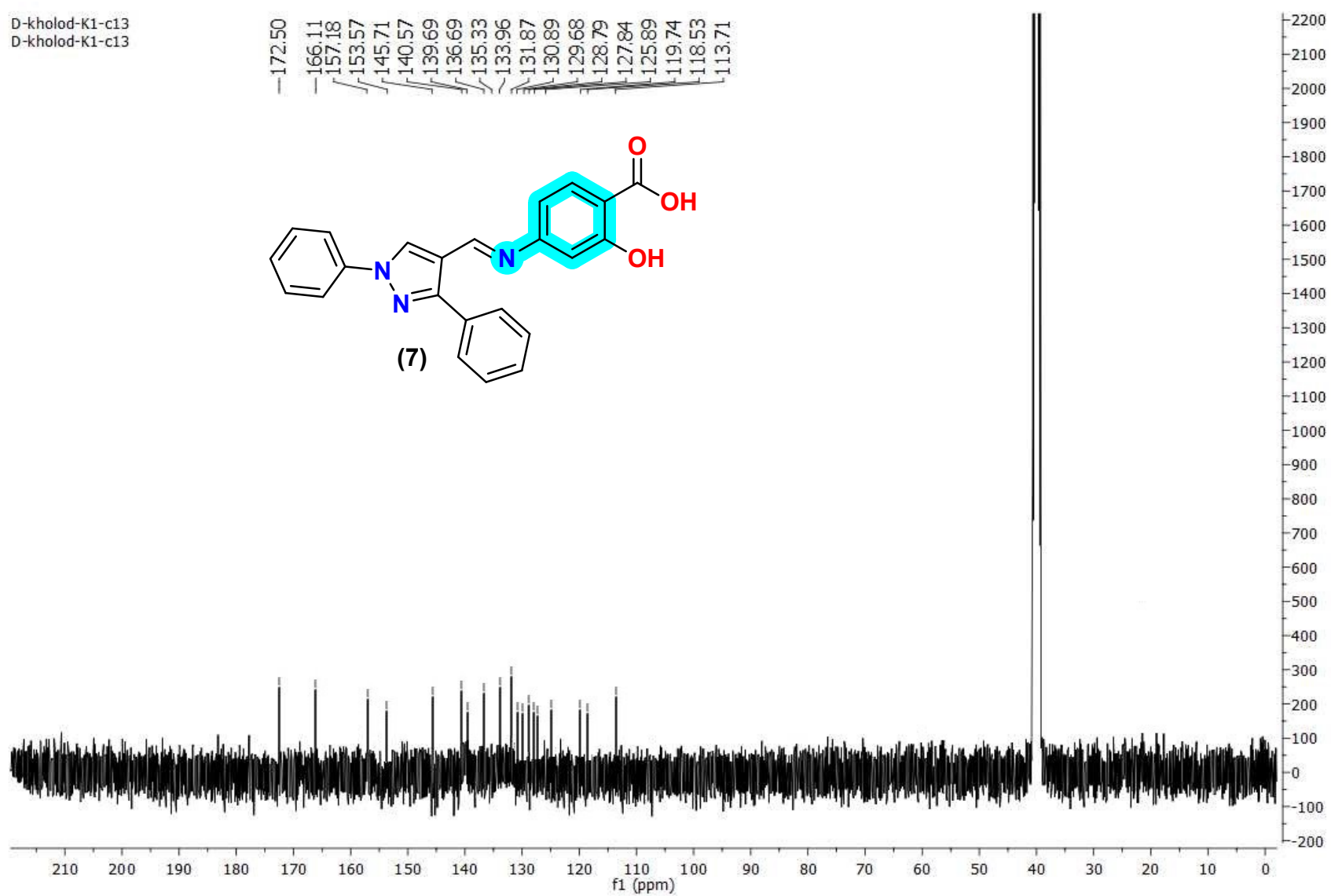


Figure (12): ¹³C NMR spectrum of compound 7

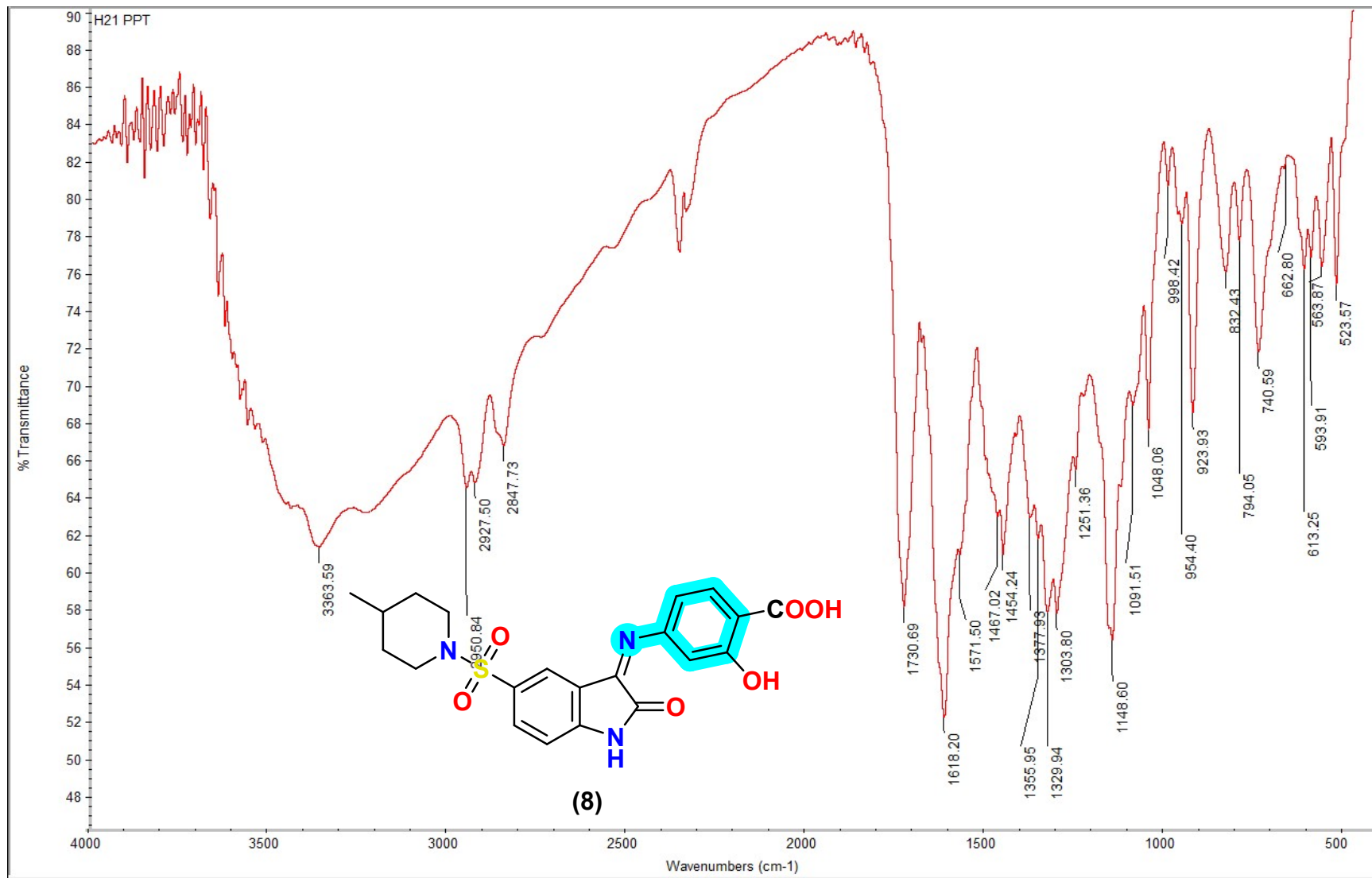


Figure (13): IR spectrum of compound 8

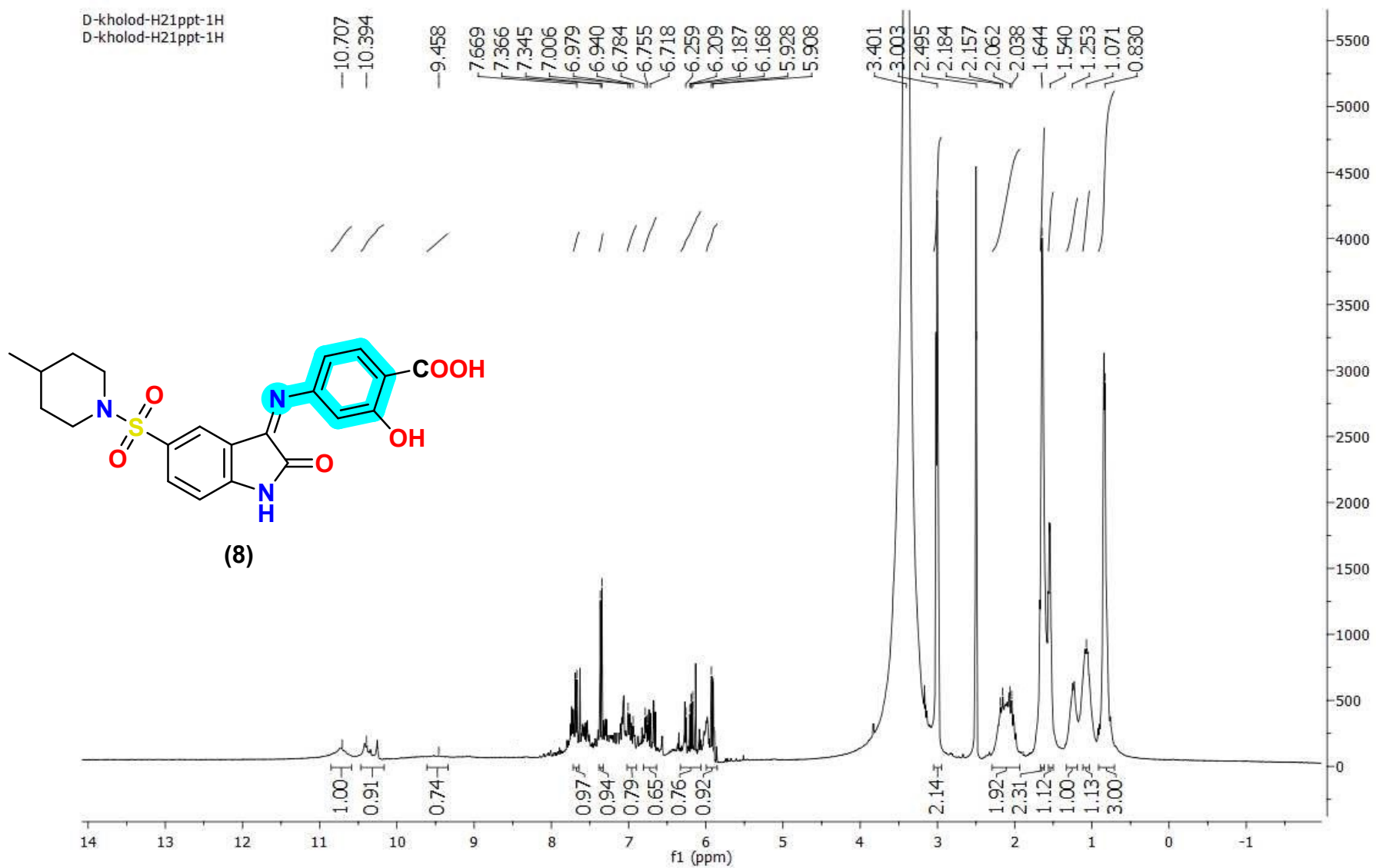


Figure (14): 1H NMR spectrum of compound 8

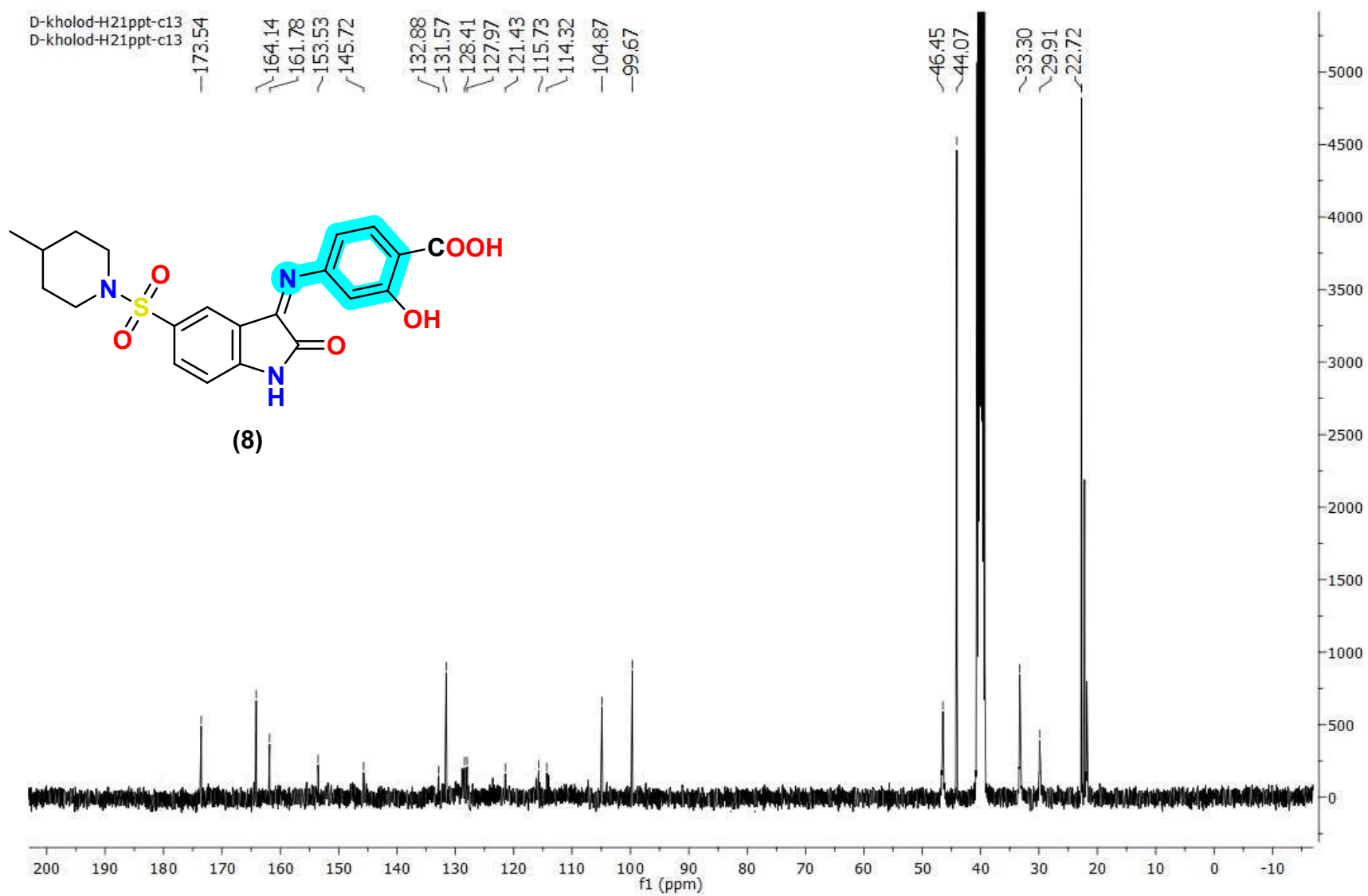


Figure (15): ^{13}C NMR spectrum of compound 8

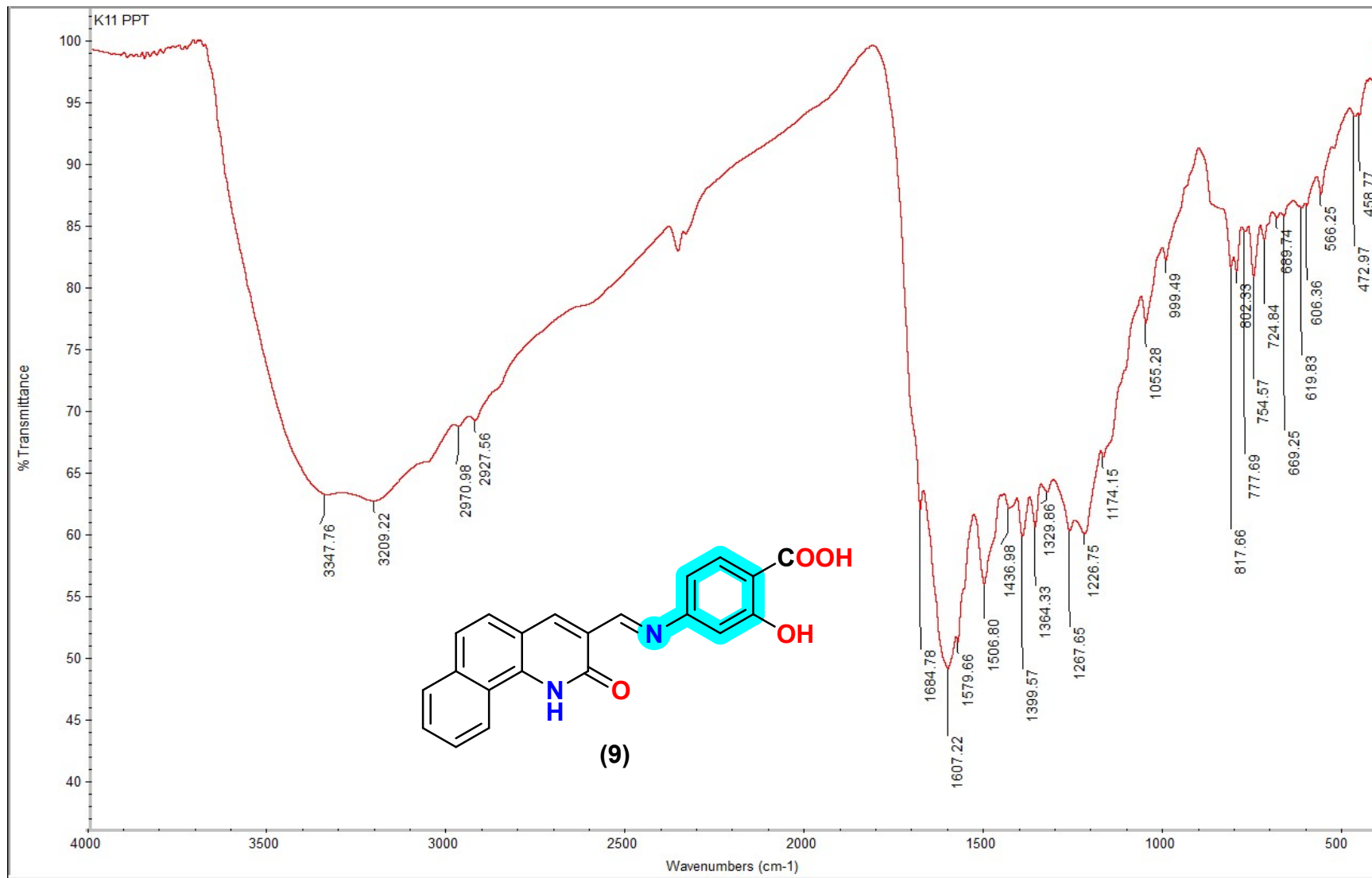


Figure (16): IR spectrum of compound 9

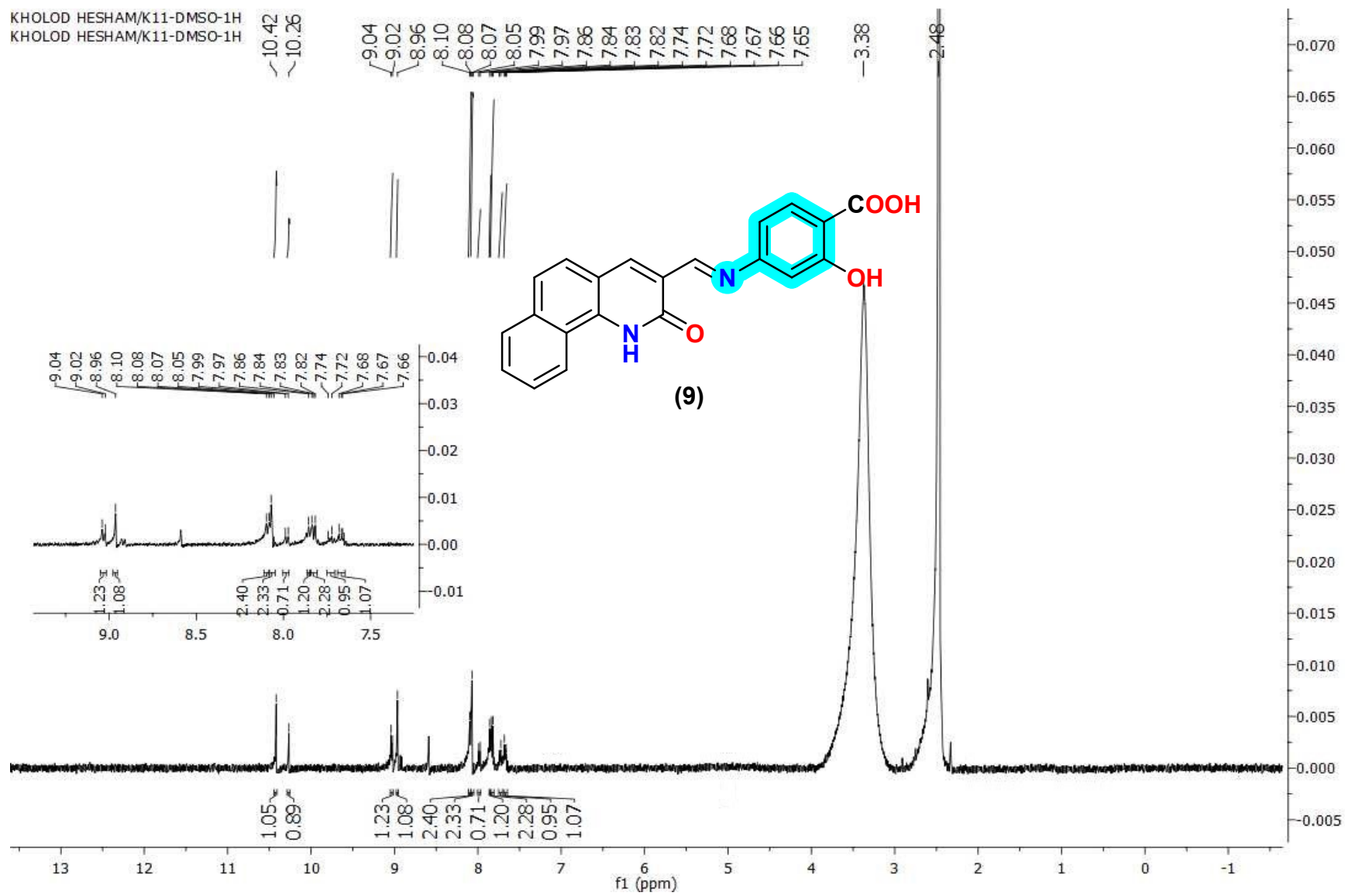


Figure (17): ^1H NMR spectrum of compound 9

D-kholod-K11-c13
D-kholod-K11-c13

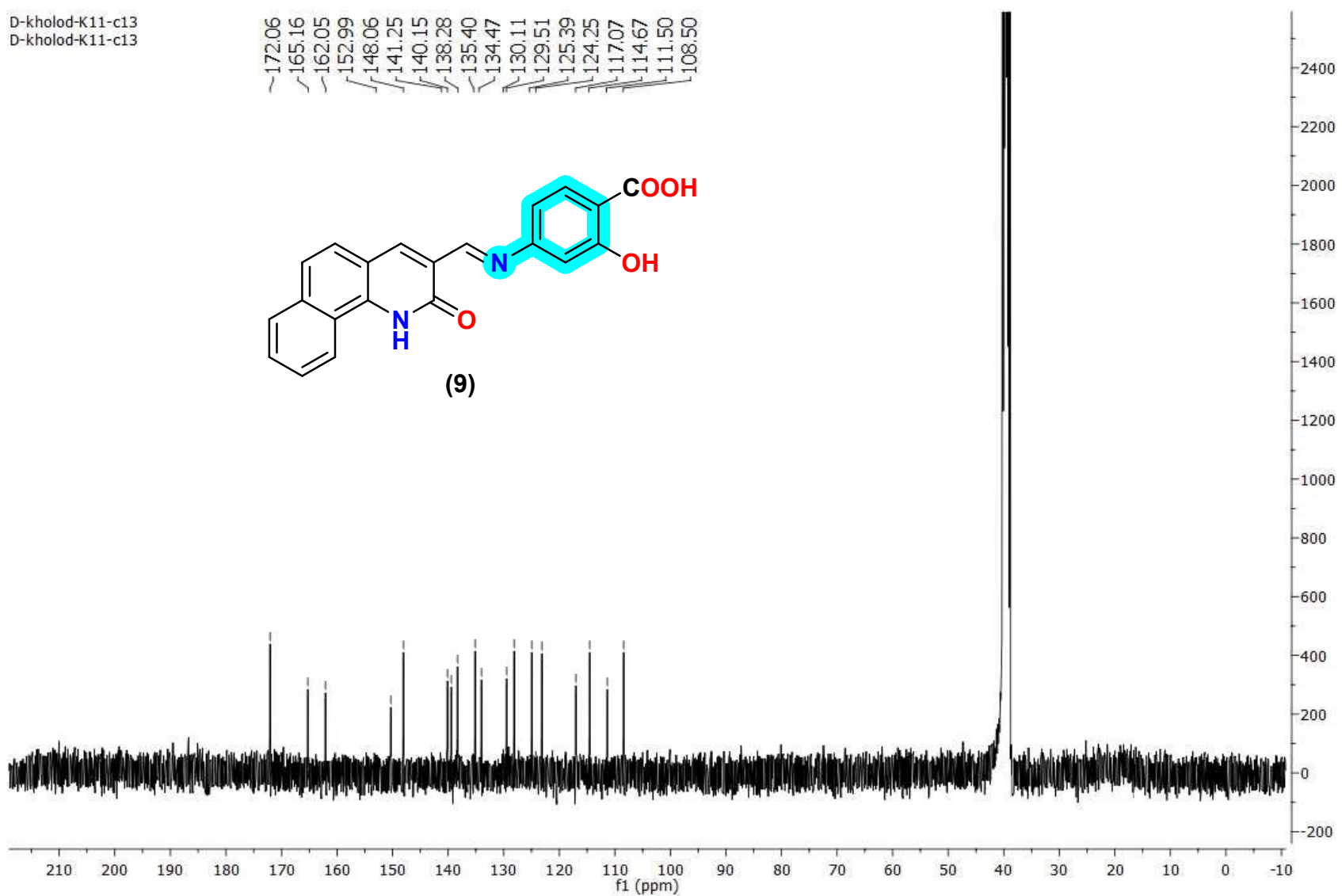


Figure (SI 18): ¹³C NMR spectrum of compound 9

3#204 RT: 3.43 P: + NL: 5.88E2
T: {0,0} + oEI Full ms [40.00-1000.00]

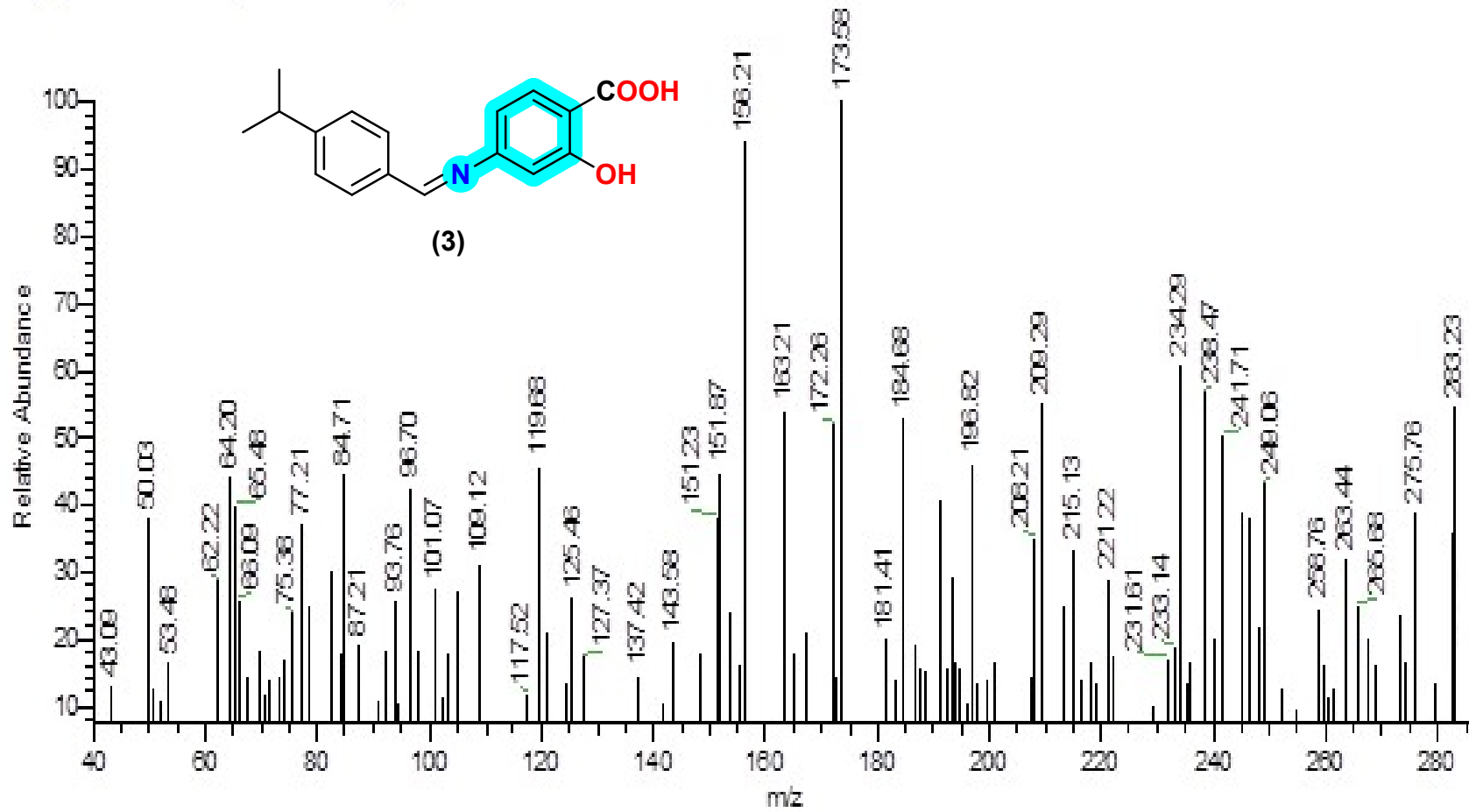


Figure (SI 19): Mass spectrum of compound 3

4 #266 RT: 4.47 P: + NL: 9.68E2
T: {0,0} + cEI Full ms [40.00-1000.00]

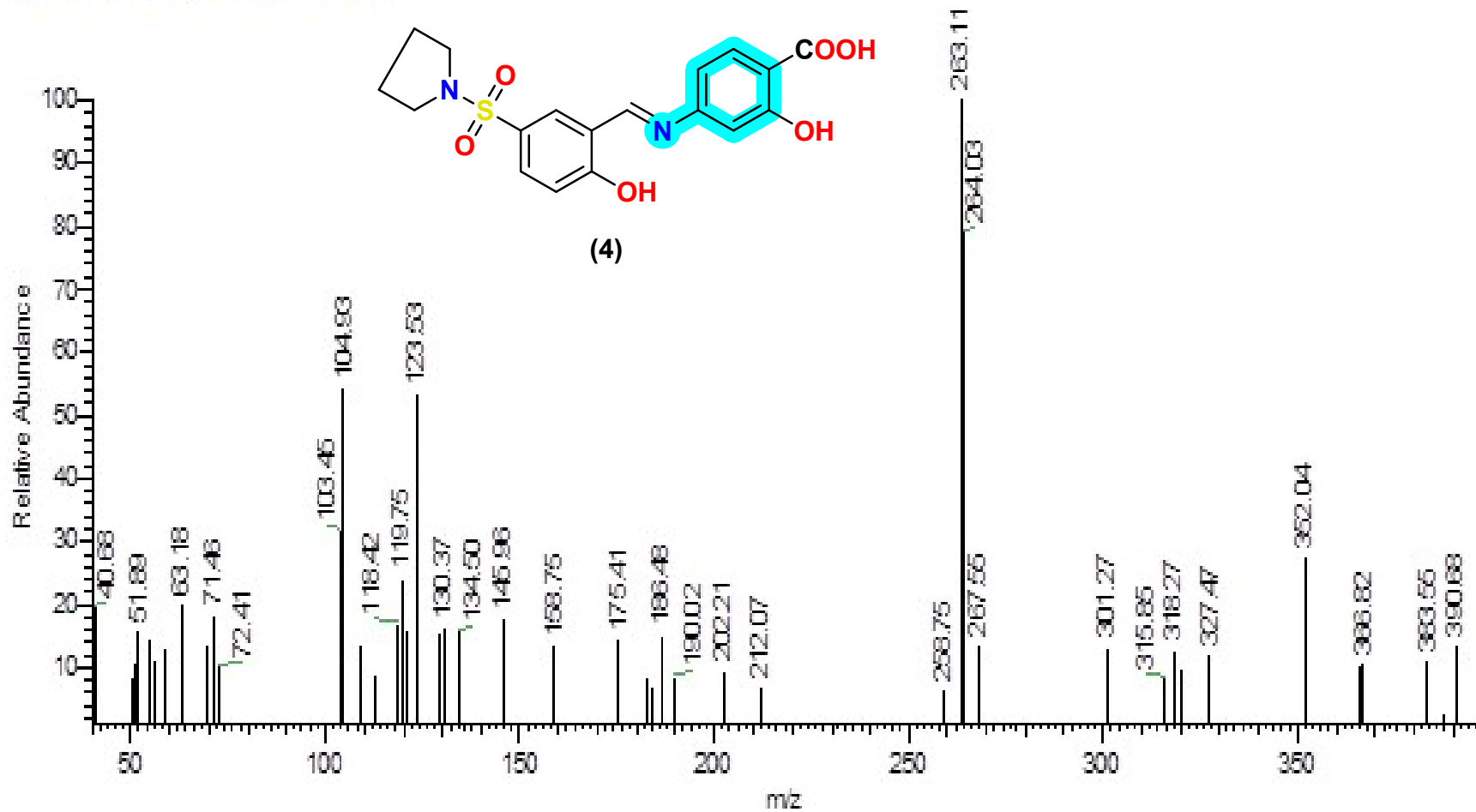


Figure (SI 20): Mass spectrum of compound 4

5#31 RT: 0.54 P: + NL: 6.02E2
T: {0.0} + cEI Full ms [40.00-1000.00]

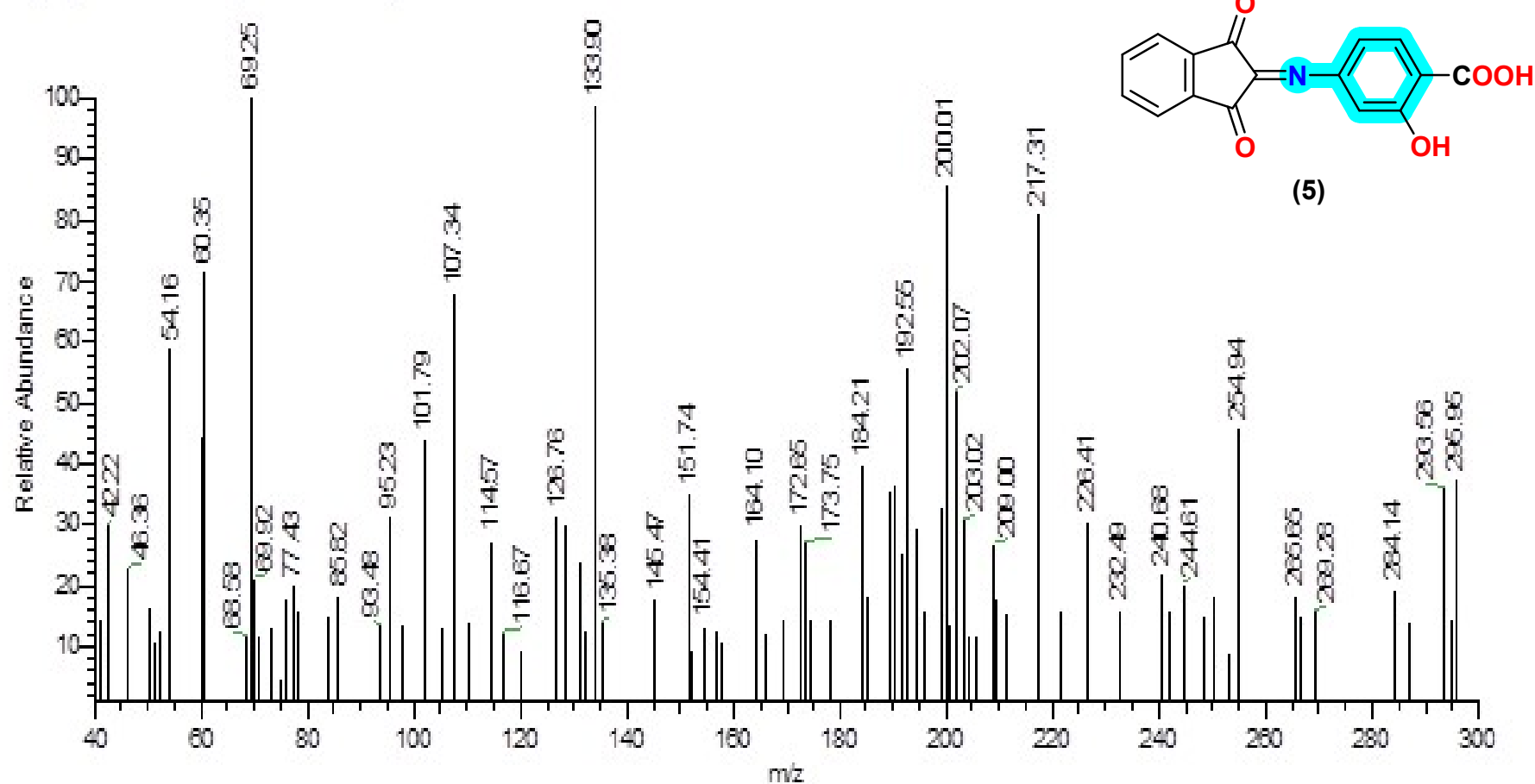


Figure (SI 21): Mass spectrum of compound 5

7 #47 RT: 0.80 P: + NL: 4.91E2
T: {0,0} + cEI Full ms [40.00-1000.00]

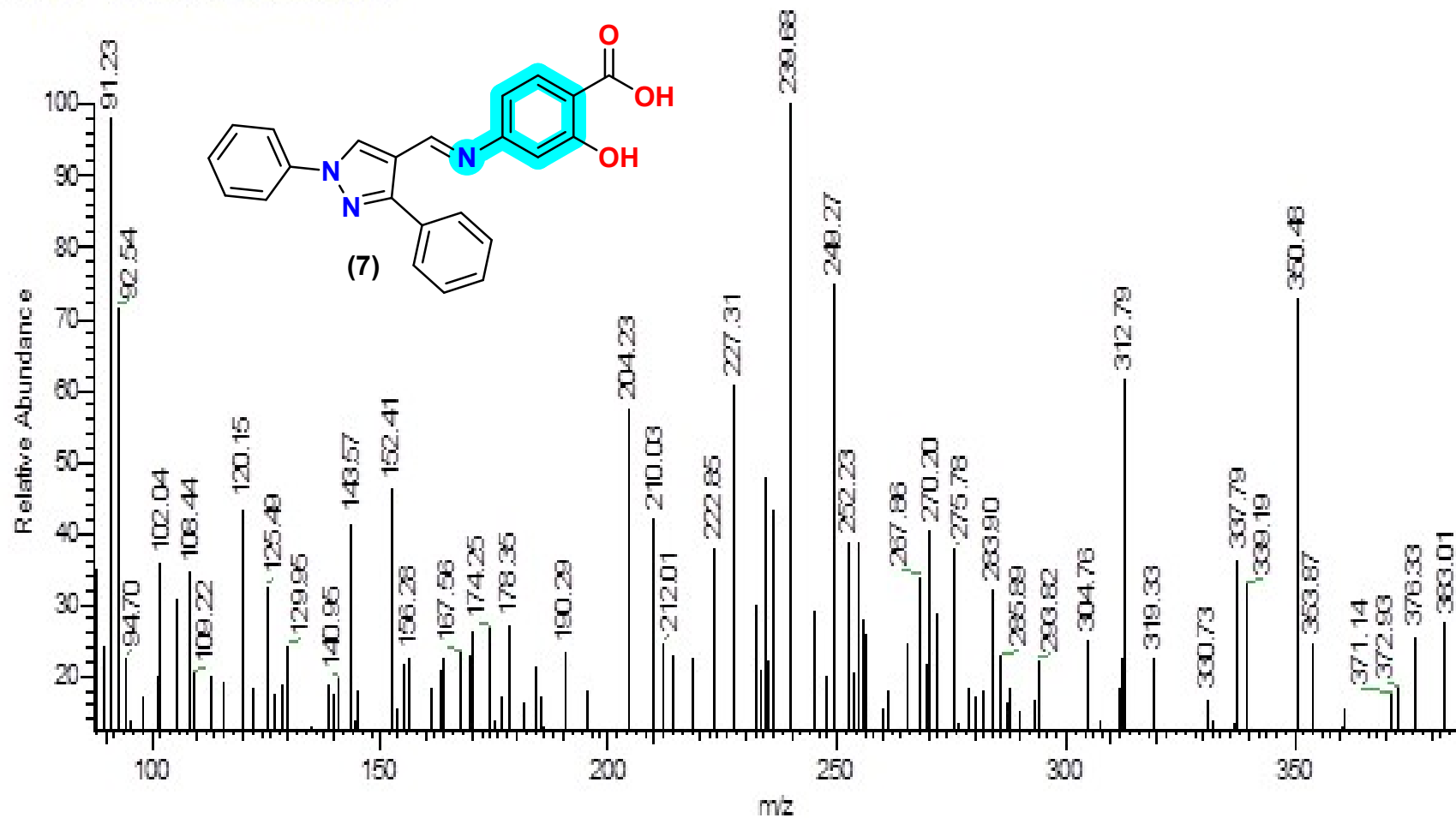


Figure (SI 22): Mass spectrum of compound 7

8 #7 RT: 0.13 Pt: + NL: 7.12E2
T: {0,0} + c EI Full ms [40.00-1000.00]

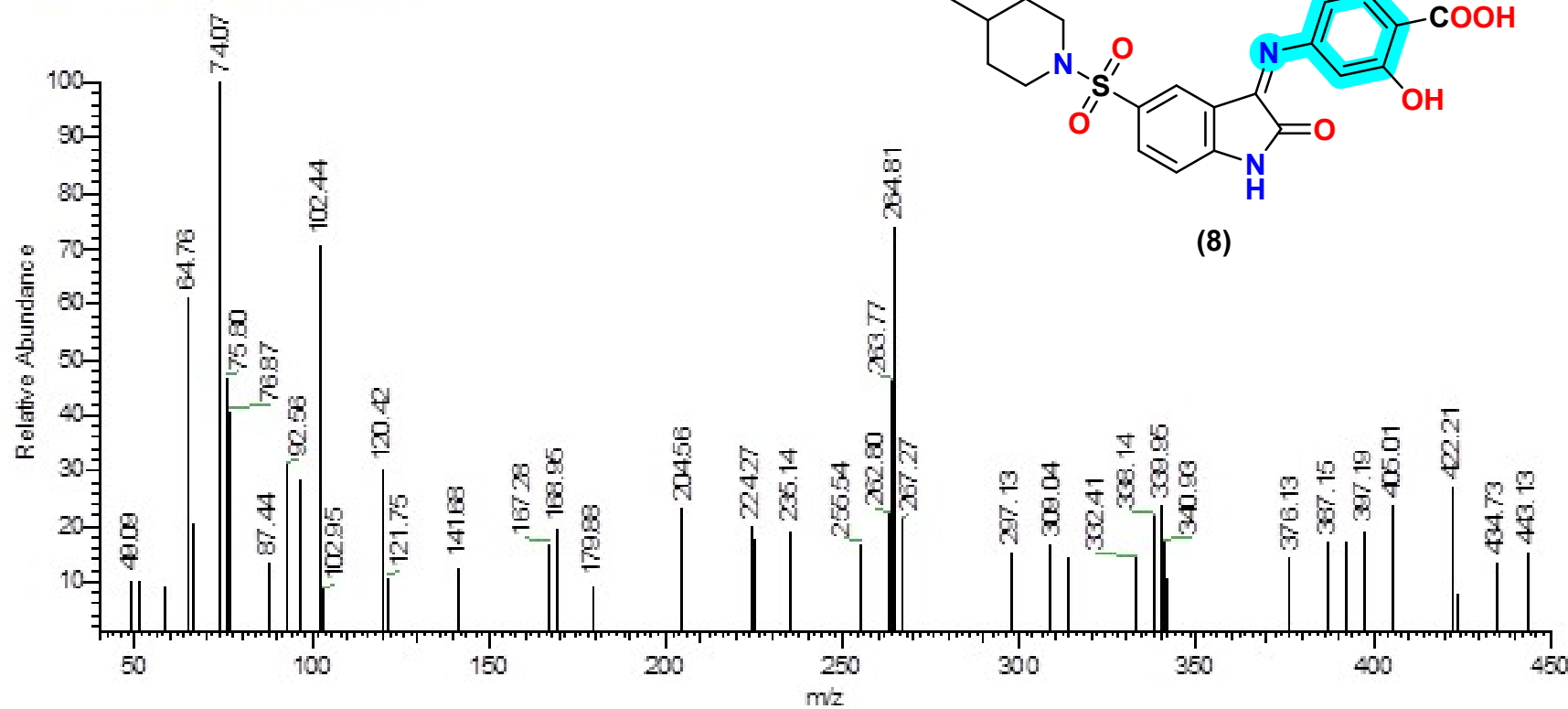


Figure (SI 23): Mass spectrum of compound 8

9#16 RT: 0.28 P: + NL: 4.15E2
T: {0,0} + c EI Full ms [40.00-1000.00]

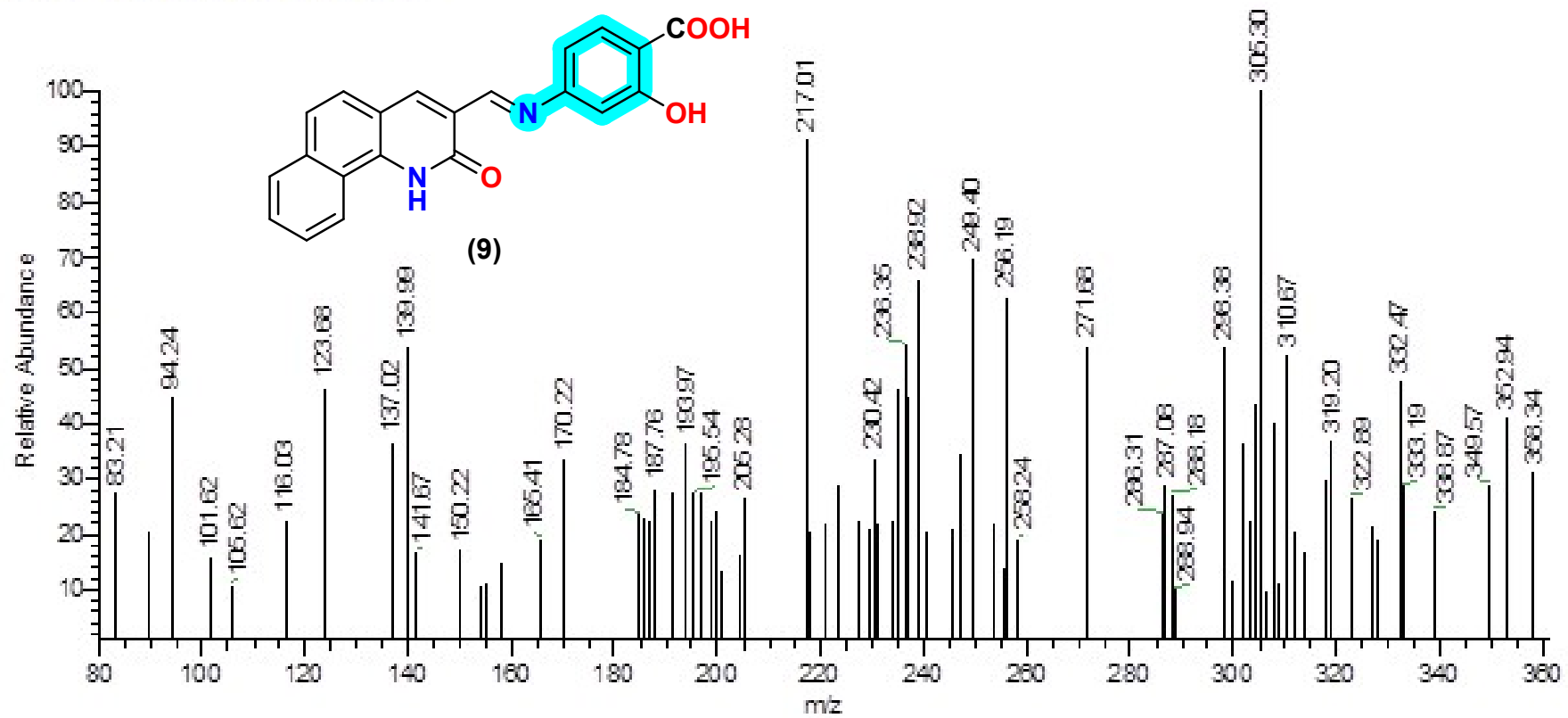


Figure (SI 24): Mass spectrum of compound 9

Toxicity profile figures

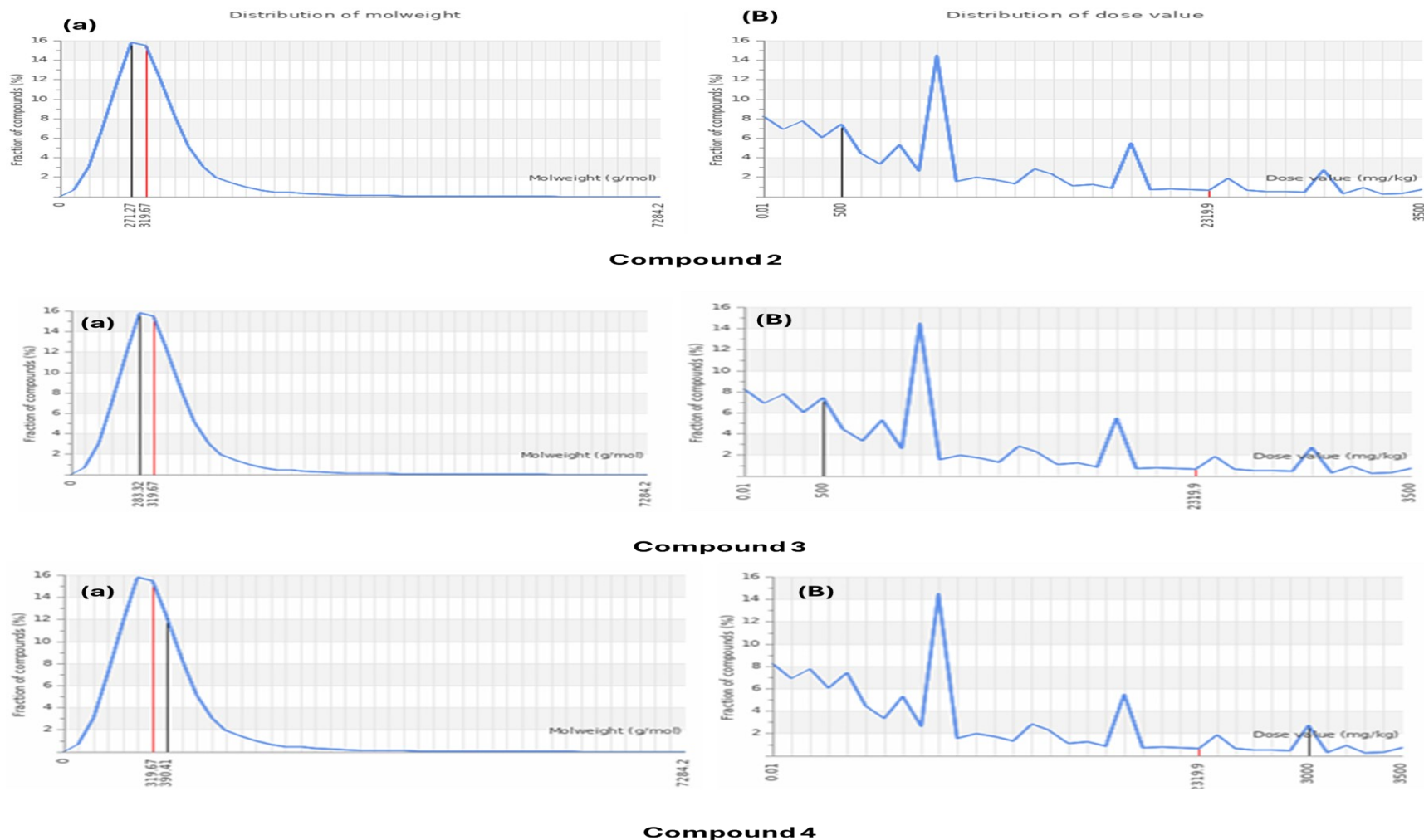


Figure (SI 25): Illustrates the physicochemical properties of compound 2, 3, and 4: (a) the distribution of molecular weight is represented by a black line compared to the mean values of the database indicated by the red line and (b) the distribution of dose value (mg/kg), where compound 7 is shown as a black line compared to the mean values of the database indicated by the red line.

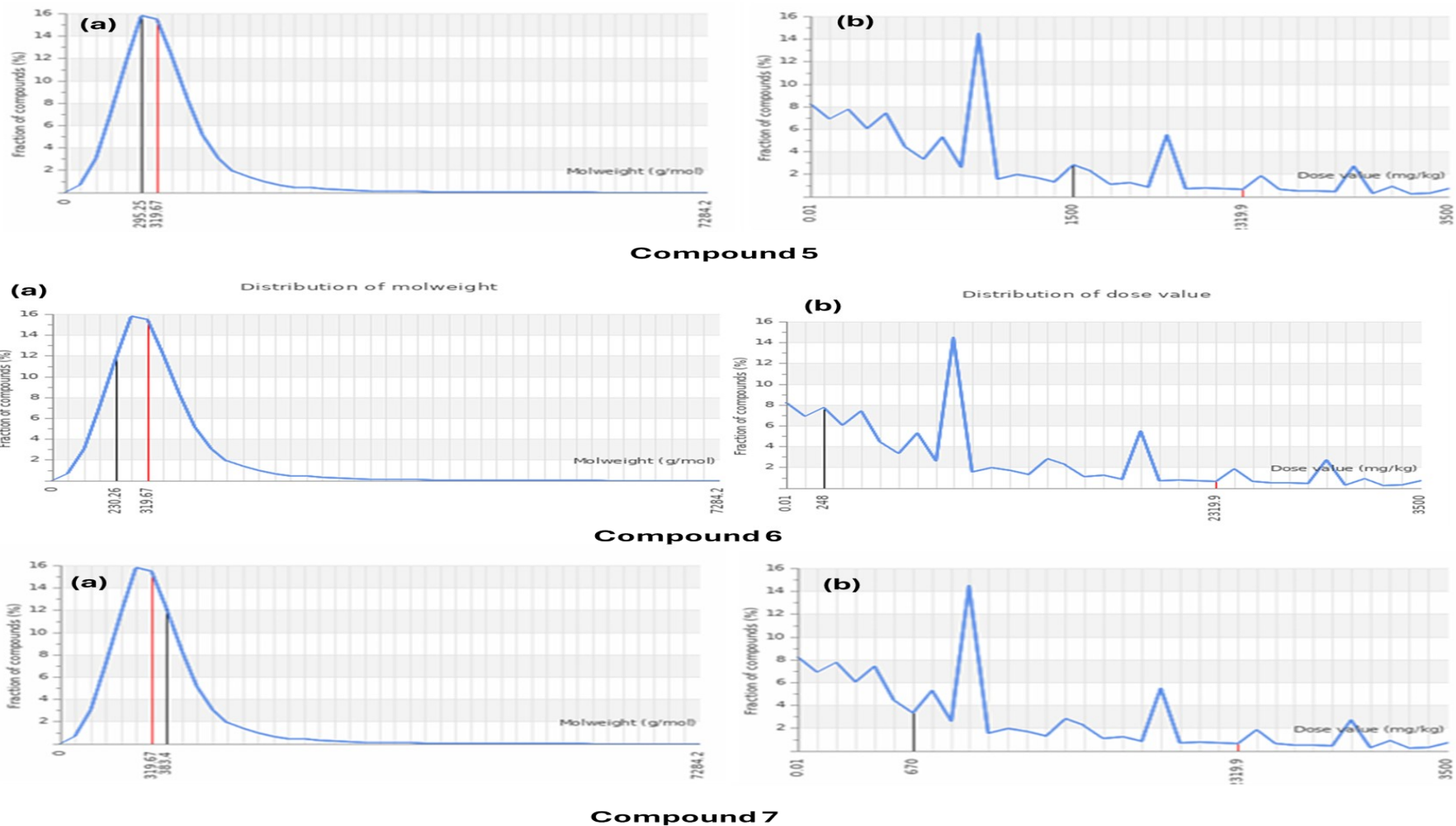


Figure (SI 26): Illustrates the physicochemical properties of compound **5**, **6**, and **7**: (a) the distribution of molecular weight is represented by a black line compared to the mean values of the database indicated by the red line and (b) the distribution of dose value (mg/kg), where compound **7** is shown as a black line compared to the mean values of the database indicated by the red line.

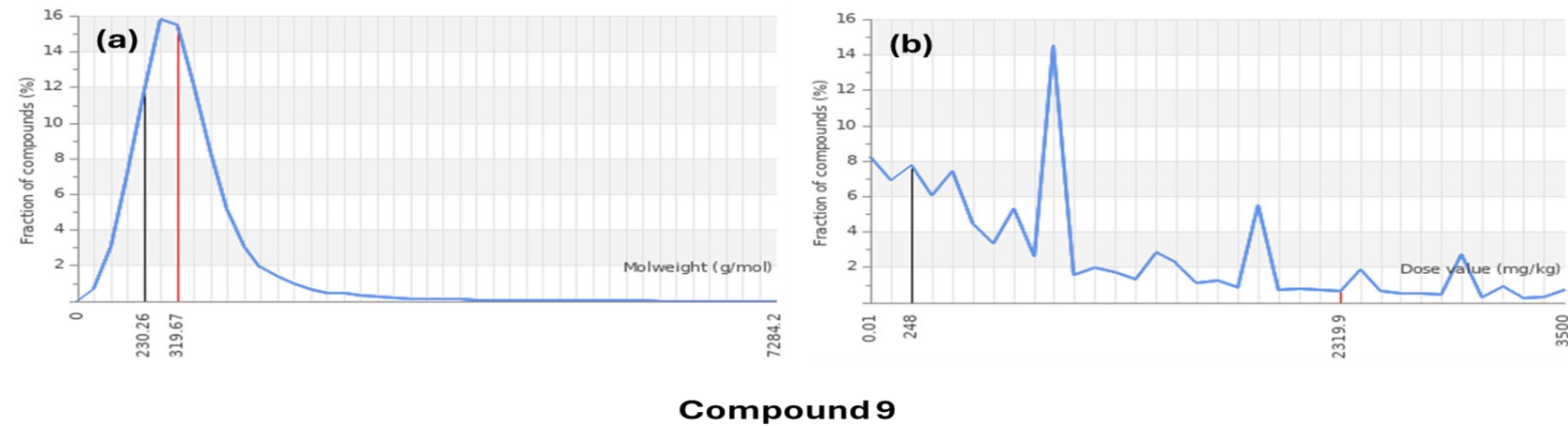
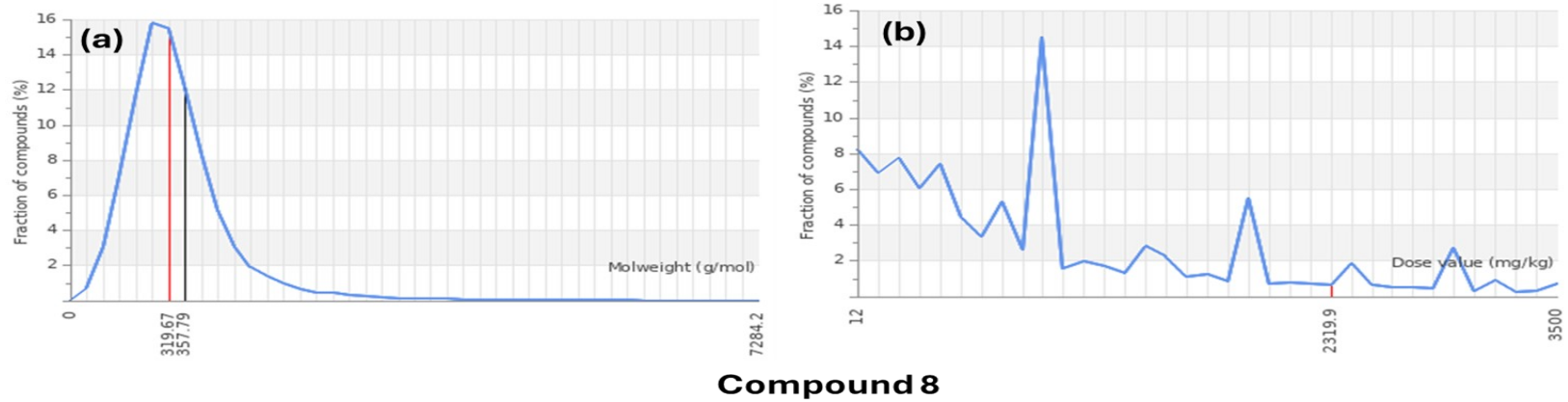


Figure (SI 27): Illustrates the physicochemical properties of compound **8** and **9** : (a) the distribution of molecular weight is represented by a black line compared to the mean values of the database indicated by the red line and (b) the distribution of dose value (mg/kg), where compound 7 is shown as a black line compared to the mean values of the database indicated by the red line.

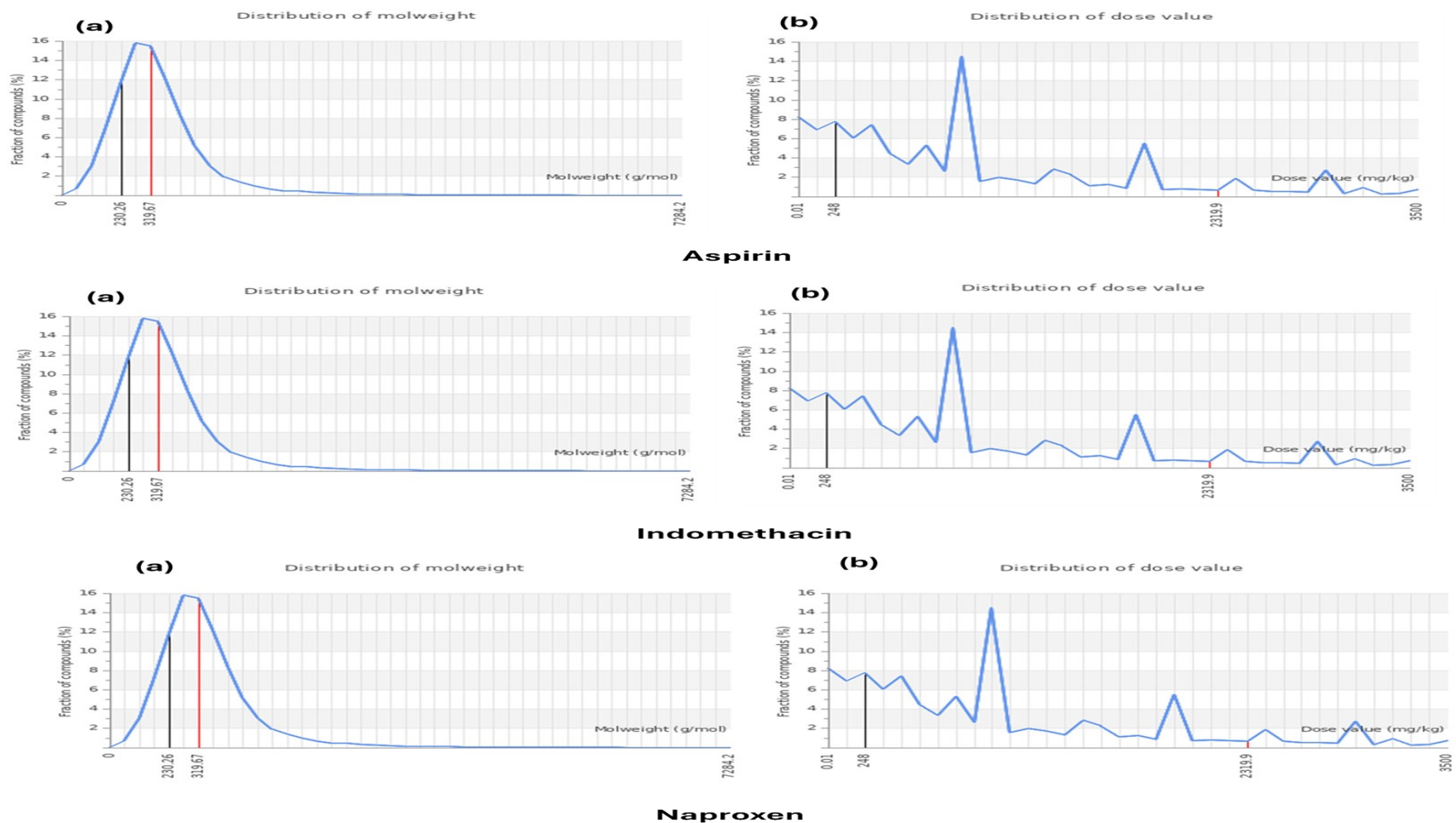


Figure (SI 28): Illustrates the physicochemical properties of **aspirin**, **indomethacin**, and **naproxen** (a) the distribution of molecular weight is represented by a black line compared to the mean values of the database indicated by the red line and (b) the distribution of dose value (mg/kg), where compound 7 is shown as a black line compared to the mean values of the database indicated by the red line.

1. *In vitro* biological activities

1.1. Anti-arthritic activity

This assay involved determining the inhibition percentage (%) of protein denaturation (**Das and Sureshkumar, 2016**) and the activity of proteinase enzyme (**Oyedapo and Famurewa, 1995**) using diclofenac sodium as the standard non-steroidal anti-inflammatory drug. The percentage of protein denaturation inhibition was measured by mixing 0.5mL of the test control solution, prepared by combining 0.45 mL of bovine serum albumin (BSA) (5% w/v aqueous solution) with 0.05 mL of distilled water. Then, 0.05 mL of each sample (at each concentration) was added to 0.45 mL of distilled water to form the product control (0.5 mL). The pH value in all prepared solutions was adjusted to 6.3 using HCl (1N). All the samples were incubated at 37 °C for 20 min, and the temperature was then increased to 57 °C, maintaining the samples at that degree for 3 min. After cooling, 2.5 mL of phosphate buffer was added to the prepared solutions. The absorbance was determined at 416 nm using a UV-Visible spectrophotometer. The percentage of protein denaturation inhibition can be calculated.

The inhibition percentage of proteinase enzyme was assessed by combining 1 mL of each sample (at each concentration) with a reaction mixture containing 0.06 mg trypsin dissolved in 1 mL of 20 mM Tris HCl buffer (pH 7.4). The mixture was then incubated for 5 minutes at 37°C, followed by the addition of 1 mL of casein (0.8% w/v). After an additional 20 minutes of incubation, 2 mL of perchloric acid (70%) was added to stop the reaction. The cloudy suspension was then centrifuged, and the absorbance of the supernatant was measured at 210 nm against buffer as the blank. The IC₅₀ of each tested sample was calculated by plotting a curve using a series of sample concentrations against the percent of proteinase inhibition.

1.2. The anti-inflammatory activity

In vitro anti-inflammatory activities were evaluated through the inhibition of two isoenzymes cyclooxygenase-1 (COX-1) and cyclooxygenase-2 (COX-2) (ovine/human) (**Alaa et al., 2016**), along with the 5-LOX enzyme (human recombinant) (**Huang et al., 2019**). The inhibition percentages of COX-1 and COX-2 were measured using the COX-1 and COX-2 kit. The inhibition percentages of 5-Lipoxygenase (5-LOX) were assessed using the 5-LOX kit. The IC₅₀ was determined *via* linear regression.

References

Alaa, A.M.; El-Azab, A.S.; Abou-Zeid, L.A.; ElTahir, K.E.; Abdel-Aziz, N.I.; Ayyad, R.R. and Al-Obaid, A.M. (2016). Synthesis, anti-inflammatory, analgesic and COX-1/2 inhibition activities of anilides based on 5, 5-diphenylimidazolidine-2, 4-dione scaffold: molecular docking studies. *Eur. J. Med. Chem.*, 115: 121-131.

Das, S. and Sureshkumar, P. (2016). Effect of methanolic root extract of *Blepharispermum subsessile* DC in controlling arthritic activity. *Research Journal of Biotechnology*, 11(4): 65-74.

Huang, Y.; Zhang, B.; Li, J.; Liu, H.; Zhang, Y.; Yang, Z. and Liu, W. (2019). Design, synthesis, biological evaluation and docking study of novel indole-2-amide as anti-inflammatory agents with dual inhibition of COX and 5-LOX. *Eur. J. Med. Chem.*, 180: 41-50.

Oyedapo, O.O. and Famurewa, A.J. (1995). Antiprotease and Membrane Stabilizing Activities of Extracts of *Fagara Zanthoxyloides*, *Olax Subscorpioides* and *Tetrapleura Tetraplera*. *Int. J. Pharmacogn.*, 33(1): 65-69.

Table SI1: All raw data for the synthesized derivatives used in our study

		S2	S3	S4	S5	S6	S7	S8	S9	Naprox	Aspirin	STD
Proteinase Inhibition (%)	1	0.77	0.72	0.73	0.86	0.73	0.86	0.79	0.77	0.24	1.10	0.20
	2	0.83	0.77	0.83	0.86	0.87	0.86	0.77	0.91	0.26	1.08	0.20
	3	0.86	0.80	0.81	0.96	0.81	0.96	0.86	1.02	0.26	1.25	0.21
COX-1	1	0.26	0.45	0.24	0.75	0.63	0.75	0.69	0.26	0.21	0.28	0.18
	2	0.25	0.46	0.24	0.73	0.74	0.73	0.66	0.25	0.20	0.28	0.18
	3	0.27	0.50	0.26	0.85	0.72	0.85	0.76	0.27	0.22	0.29	0.19
COX-2	1	0.21	0.38	0.20	0.58	0.50	0.58	0.53	0.21	0.17	0.23	0.15
	2	0.21	0.38	0.20	0.58	0.58	0.58	0.52	0.21	0.17	0.24	0.15
	3	0.21	0.39	0.20	0.63	0.54	0.63	0.57	0.21	0.17	0.23	0.15
5-LPO	1	0.37	0.66	0.35	1.31	1.05	1.31	1.16	0.36	0.29	0.41	0.25
	2	0.37	0.72	0.35	1.27	1.29	1.27	1.10	0.37	0.29	0.41	0.26
	3	0.39	0.79	0.37	1.52	1.21	1.51	1.30	0.38	0.30	0.42	0.26

Table SI2: Data of the cytotoxic activity of the different synthetic compounds against human normal human fibroblast (BJ-1) cell line compared to Doxorubicin as standard.

Sample 2						
Conc. (μg/mL)	0.00	31.13	62.50	125.00	250.00	500.00
Mean OD	0.38	0.30	0.24	0.17	0.11	0.04
Viability %	98.15	90.63	83.11	75.59	68.07	60.55
IC₅₀ (μg/mL)	169.05 ± 8.50					
Sample 4						
Conc. (μg/mL)	0.00	31.13	62.50	125.00	250.00	500.00
Mean OD	0.36	0.31	0.28	0.19	0.11	0.07
Viability %	95.78	88.26	80.74	73.22	65.70	58.18
IC₅₀ (μg/mL)	157.40 ± 13.17					
Sample 9						
Conc. (μg/mL)	0.00	31.13	62.50	125.00	250.00	500.00
Mean OD	0.36	0.31	0.28	0.19	0.11	0.07
Viability %	92.85	85.33	77.81	70.29	62.77	55.25
IC₅₀ (μg/mL)	121.49 ± 7.94					
DOX						
Conc. (μg/mL)	0.00	6.25	12.50	25.00	50.00	100.00
Mean OD	0.27	0.23	0.17	0.13	0.09	0.80
Viability %	98.75	91.23	83.71	76.19	68.67	61.15
IC₅₀ (μg/mL)	39.75 ± 2.86					